A Thesis on

SINTERING OF CEMENT CONCRETE AND ALKALI ACTIVATED CONCRETE

Submitted by

ARPAN DAS

in Partial Fulfilment for Award of the Degree of

MASTER OF ENGINEERING IN CIVIL ENGINEERING

Specialisation in

Structural Engineering

Class Roll No.-002210402026

Examination Roll No.- M4CIV24023

University Registration No.- 139623 of 2017-2018

Under the Guidance of

Prof. Dr. AMIT SHIULY

DEPARTMENT OF CIVIL ENGINEERING

FACULTY OF ENGINEERING AND TECHNOLOGY

JADAVPUR UNIVERSITY

AUGUST 2024

DECLARATION

This thesis titled **"SINTERING OF CEMENT CONCRETE AND ALKALI ACTIVATED CONCRETE"** prepared and submitted in the partial fulfilment of the requirements for the degree of Master of Civil Engineering (with specialisation in Structural Engineering) at Jadavpur University for the academic session 2023-2024.

Date: 27/08/2024

Place: Civil Engineering Department,

Jadavpur University, Kolkata.

Arpan Das

ARPAN DAS

Master of Civil Engineering

(Structural Engineering)

2nd Year 2nd Semester

Class Roll No.- 002210402026

University Registration No.- 139623 of 2017-2018

JADAVPUR UNIVERSITY

DEPARTMENT OF CIVIL ENGINEERING

KOLKATA – 700032

RECOMMENDATION CERTIFICATE

It is hereby certified that this thesis titled **"SINTERING OF CEMENT CONCRETE AND ALKALI ACTIVATED CONCRETE"** has been prepared and submitted in the partial fulfilment for the degree of **Master of Civil Engineering (with specialisation in Structural Engineering)** at **Jadavpur University** by **ARPAN DAS (Class Roll No.-002210402026)**, a student of 2nd year of the said course for the session 2023-2024, has carried out this work under my supervision and guidance.

I hereby approve this report for submission and presentation.

Amit Shiuly 27.8.24.

Dr. AMIT SHIULY
Associate Professor
Department of Civil Engineering
Jadavpur University

Associate Professor
Department of Civil Engineering
Jadavpur University
Kolkata-700 032

Countersigned by

Dipak Laha 27.8.24

Dean
Faculty of Engineering and Technology
Jadavpur University

DEAN
Faculty of Engineering & Technology
JADAVPUR UNIVERSITY
KOLKATA-700 032

Partha Bhattacharyya 27/8/24

Head of the Department
Department of Civil Engineering
Jadavpur University

Head
Department of Civil Engineering
Jadavpur University
Kolkata-700 032

JADAVPUR UNIVERSITY

DEPARTMENT OF CIVIL ENGINEERING

KOLKATA – 700032

CERTIFICATE OF APPROVAL

This is to certify that this thesis is hereby approved as an original work conducted and presented satisfactorily to warrant its acceptance as a prerequisite to the degree for which it has been submitted. It is implied that by this approval the undersigned do not necessarily endorse or approve any statement made, opinion expressed conclusion drawn therein, but approve the thesis only for the purpose for which it is submitted.

Final Examination for Evaluation of Thesis:

1. _____

2. _____

3. _____

(Signature of Examiners)

*Only in case the thesis is approved

ACKNOWLEDGEMENT

I would like to express my special thanks of gratitude to my guide **Dr. Amit Shiuly,** Associate Professor, Department of Civil Engineering, Jadavpur University for giving me the golden opportunity to do this work on **"SINTERING OF CEMENT CONCRETE AND ALKALI ACTIVATED CONCRETE"** and support in my thesis work.

I am grateful to all the professors of Civil Engineering Department of Jadavpur University who helped me a lot. It is only their constant suggestion that I have been able to finish my thesis work.

I am thankful to my family members for always standing by my side. Their blessings , motivation and inspiration have always provided me a high mental support. I am also thankful to my classmates for their assistance and cooperation during the course.

Date: 27/08/2021

Place- Civil Engineering Department,

Jadavpur University

Arpan Das.

Arpan Das

Contents

List of Tables

List of Figures

ABSTRACT

Concrete, as the backbone of modern infrastructure, plays a crucial role in the construction industry, yet its environmental impact, primarily due to the high CO_2 emissions associated with Portland cement production, necessitates the exploration of more sustainable alternatives. Alkali Activated Concrete (AAC) has emerged as a promising substitute, offering reduced environmental footprints. This thesis investigates the effects of sintering techniques on the mechanical and durability properties of both traditional Cement Concrete (CC) and Alkali Activated Concrete (AAC). It is to be mentioned that, sintering, a technique involving the compaction and solidification of materials through the application of heat and pressure, was explored to enhance the properties of these concrete types. In this study, concrete specimens of varying grades (M20, M25, M30) were prepared and subjected to different sintering conditions, including normal conditions, application of 20 kN pressure, and a combined condition of 100°C for 5 minutes under 20 kN pressure. The performance of the concrete was rigorously evaluated through a series of tests, including compressive strength, split tensile strength, Rebound Hammer Test, Ultrasonic Pulse Velocity (UPV) Test, sorptivity, and Rapid Chloride Permeability Test (RCPT). Additionally, the microstructural characteristics were analysed to understand the underlying changes brought about by the sintering process. The results of this study reveal that sintering significantly enhances the compressive and split tensile strengths, as well as the durability characteristics, of both CC and AAC. Notably, AAC consistently exhibited superior performance compared to CC, particularly under optimized sintering conditions. The findings underscore the potential of sintering techniques not only to improve the mechanical properties and durability of concrete but also to contribute to the development of more sustainable and high-performance construction materials. This research provides a valuable contribution to the field, highlighting the viability of sintering as a method to optimize concrete formulations, thereby advancing sustainable practices within the construction industry.

Chapter 1

1.Introduction

1.1. General

Concrete, essential to modern construction, ranks as the world's second most consumed material after water, with Portland cement serving as its primary binder [1]–[5]. As the construction sector grows and the demand for building materials increases, concrete—comprising cement, aggregates, and water—remains the predominant choice. However, Portland cement production is a significant environmental concern, responsible for nearly 8% of global CO_2 emissions each year[6]–[9]. In response to this challenge, the industry is increasingly focusing on sustainable alternatives like alkali-activated materials (AAMs), which offer a viable substitute for conventional Portland cement[10][11]. These materials are created by activating aluminosilicate or calcium aluminosilicate precursors in highly alkaline environments. [12]–[15] Geopolymers, a specific type of AAM, are particularly noteworthy; they are produced by synthesizing aluminosilicate sources such as metakaolin or fly ash with alkaline activators like sodium hydroxide paired with sodium silicate or potassium hydroxide with potassium silicate, forming a robust three-dimensional polymeric network[16]–[18].

Cement concrete(CC), made from Portland cement, water, and aggregates, is the traditional material used in construction due to its well-known mechanical properties, durability, and lower cost. However, its production is energy-intensive and contributes significantly to global CO_2 emissions. In contrast, alkali-activated concrete (AAC) is a more sustainable alternative that uses industrial by-products like fly ash or slag, activated with alkaline solutions[10][19][20]. AAC often exhibits superior mechanical properties, such as higher compressive strength and better resistance to chemical attacks, making it more durable, especially in harsh environments. Despite its potential environmental benefits and enhanced performance, AAC faces regulatory, supply chain challenges and requires specific raw materials and curing conditions[10]. While CC remains widely used due to its availability and established cost structure, AAC offers a promising, eco-friendly option for projects prioritizing sustainability and durability under challenging conditions.

1.2 Sintering Effect

Sintering is a critical process in material science and engineering that involves compacting and solidifying materials through the application of pressure or heat without reaching the melting point[21]. This process is essential in various manufacturing industries, including steelmaking[22]–[30], ceramics[31]–[40], plastics[41]–[49], self-lubricating bearings[50]–[57], and electrical contacts[58], [59]. The core mechanism of sintering lies in the diffusion of nanoparticles across particle boundaries, leading to the fusion of particles and the formation of a solid mass known as sinter[60][61]. The driving force behind sintering is the reduction of the total free energy, which results in the material reaching a more stable, minimal energy state[62]. The effectiveness of sintering is often measured by its ability to reduce porosity and improve material properties, such as strength, electrical conductivity, translucency, and thermal conductivity. This process is vital in a wide range of applications, from traditional materials like ceramics to emerging fields such as sustainable building materials [63]–[66].

1.3. Need for Present Study

The sintering process is essential for creating sustainable building materials, with "hot-pressing" techniques producing exceptionally high strengths. Intermediate strength levels can be achieved by applying high pressures at room temperature to Portland cement pastes. The cement industry, responsible for about 8% of global CO2 emissions and significantly contributing to global warming, can benefit from alkali-activated concrete (AAC) as a more sustainable alternative. AAC utilizes industrial waste like fly ash, reducing reliance on traditional Portland cement and thus decreasing CO2 emissions. Although AAC typically requires several days to weeks to cure and has lower mechanical properties, it is cost-effective, energy-efficient, thermally stable, and environmentally friendly. By incorporating pozzolanic materials such as fly ash, ground granulated blast furnace slag (GGBFS), and rice husk ash, AAC reduces carbon footprints and enhances sustainability. AAC boasts superior physical, mechanical, and durability characteristics, including high resistance to acid, sulphate, and salt attacks, making it suitable for a variety of construction applications including bridges, high-rise buildings, highways, and hydraulic structures. The adoption of AAC supports sustainable development by minimizing CO2 emissions, optimizing resource use, and utilizing waste materials. Additionally, using cold reaction sintering—an alternative to traditional high-temperature sintering—can produce high-strength hardened bodies in a much shorter time

(within minutes) and at lower temperatures (<200°C), thus saving energy and promoting overall sustainability.[67]

1.4. Objective and Scope of Work

The objective of this study is to explore the potential of sintering techniques to improve the properties of alkali activated concrete and cement concrete. The scope of work includes several steps which are to be followed in this experimental study.

The steps are:

1. Mix Design of cement concrete (as per IS 10262-2019)
2. Mix Design of alkali activated concrete (as per IS 17452 : 2020)
3. Casting and Sintering process will be done on done.
4. Study of compressive, split tensile strength of the specimen.
5. Study of Non Destructive tests(Rebound Hammer Test, Ultrasonic Pulse Velocity (UPV) test) of the specimen.
6. Study of durability by Water Absorption (Sorptivity) Test, RCPT (Rapid Chloride Penetration Test).
7. Microstructural study by Optical Microscope using Image J software.

1.5. Organization of Thesis

The thesis has been divided into five chapters. The tables and figures are presented in a sequence as they appear in the text.

In Chapter 1 an attempt has been made to introduce the problem along with the need for present research, scope and objectives of the work and organization of thesis.

In Chapter 2 a detailed literature review on the relevant topic is given.

In Chapter 3 experimental programmes that are carried out in the laboratory are presented.

In Chapter 4 detailed discussions in regard to test results obtained are furnished.

In Chapter 5 concluding remarks along with major findings, limitations and future scope of study is depicted.

References are given at the end.

Chapter 2

2.Literature Review

2.1. Materials Used

The literature review reveals a comprehensive understanding of sintering processes, with a specific focus on its applications in building materials, notably Geopolymer Concrete (GPC). Previous studies have explored the effects of sintering on conventional cements and its potential to enhance material properties. Notably, the high strengths achieved through hot pressing pastes highlight the viability of sintering in cement-based materials.

The need for sustainable building materials is addressed through the exploration of alkali-activated concrete, such as GPC, which utilizes industrial waste like fly ash[68]–[77], contributing to reduced carbon footprints. GPC emerges as an alternative to traditional Portland cement concrete, showcasing better physical, mechanical, and durable properties. The literature emphasizes the role of sintering in expediting the curing process for alkali-activated concrete, presenting a novel approach for achieving high strength in a shorter duration.

Geopolymer concrete is typically composed of industrial by-products such as fly ash[68]–[77], slag, or metakaolin[78]–[87], which are rich in aluminosilicate minerals. Other materials which can be used are agro ash[88]–[97], calcined clay[98]–[106], GGBS(Ground Granulated Blast Furnace Slag)[107], [108], [117], [109]–[116] ,red mud[118], [119], [128], [129], [120]–[127] , rice husk ash[130]–[139], silica fume[140], [141], [150], [142]–[149], volcanic ash[151], [152], [159], [152]–[156], [156]–[158] .These materials serve as the precursor for the geopolymer binder. The process involves the activation of these materials with alkaline solutions, usually sodium hydroxide (NaOH) and sodium silicate (Na_2SiO_3), to initiate a chemical reaction that forms a three-dimensional polymeric network.

Studies on various materials, including fly ash, diatomite, and slag, showcase the diverse applications of sintering in improving their properties for construction purposes. The literature review underscores the economic, energy-efficient, and environmentally friendly attributes of Geopolymer Concrete, positioning it as a potential solution for sustainable construction.

While existing research provides valuable insights, there is a notable gap in exploring the durability characteristics of sintered cement and alkali-activated concrete. Additionally, further investigations into the long-term compressive strength and potential reactions in sintered

concrete are identified as areas requiring more attention. The literature review sets the stage for the present study, which aims to address these gaps and contribute to the evolving landscape of sustainable construction materials.

In Table 2.1, diverse materials and methodologies for making cement concrete are presented. Researchers like Roy, Gouda, and Bobrowsky (1972) [160] utilized a hot press cell for cylindrical specimens subjected to high pressures and temperatures. Others, such as Posi et al. (2013) [161], explored the sintering treatment of fly ash under different conditions. Meanwhile, Eskandari-Naddaf and Azimi-Pour (2018) [162] prepared dry pressed concrete samples with varying strength grades. Notably, Sumarni and Wijanarko (2018) [163] incorporated unconventional materials like rice straws as concrete brick fillers. In Table 2.2, materials for alkali-activated concrete are discussed. Researchers like Ranjbar et al. (2017) [164] used low calcium fly ash activated by a mixture of sodium silicate and sodium hydroxide. Wang et al. (2019) [165] explored metakaolin and fly ash activation, while Cao et al. (2023) [166] manufactured fly-ash-based strain-hardening geopolymer composite plates through hot-pressing. These studies collectively contribute to the understanding of material selection and processing techniques in the development of both traditional and alkali-activated concrete.

Table 2.1: Materials used for making Cement Concrete

Sl. No.	Researchers	Materials used
1.	Roy, Gouda and Bobrowsky, (1972) [160]	All specimens were cylindrical with a nominal diameter of 1/2" , prepared in specialized cells. A custom hot press cell was designed to compress samples of 1/2" diameter and up to 1" in height from both ends, capable of withstanding internal pressures exceeding 100,000 psi at 950°C, equipped with seal rings to prevent material leakage.
2.	Roy and Gouda, (1973)[167]	Two pressure cells, 1/2" diameter x 1/2" or 1" long cylindrical specimens.
3.	Mangialardi, (2001)[168]	The study tested four types of fly ash from various Italian MSW incineration plants. Sintering was carried out on untreated and washed fly ash, using cylindrical specimens (15 mm diameter, 20 mm height) subjected to varying compact pressures, sintering temperatures, and durations.
4.	Posi et al., (2013)[161]	Ordinary Portland Cement (OPC) and diatomite sourced from Lampang province in northern Thailand were used in the study. The

		diatomite was crushed and calcined at temperatures of 400, 600, 800, and 1000°C for 4 hours, then classified into fine aggregate (FA), medium aggregate (MA), and coarse aggregate (CA) with particle sizes ranging from 0.001 to 1.18 mm, 1.18 to 4.75 mm, and 4.75 to 12.5 mm, respectively.
5.	Wang et al., (2016)[165]	Dynamic biaxial compressive tests were conducted on dam concrete cubes with a 250 mm edge length, both in dry and saturated conditions. These experiments were performed using a large-scale static and dynamic triaxial electro-hydraulic servo multiaxial testing system.
6.	Xue et al., (2016)[169]	The materials used included BOF (Basic Oxygen Furnace) slag, gypsum, and chemically pure substances such as CaO, SiO_2, Al_2O_3, $CaSO_4$, and H_3BO_3. All materials were ground into powders with particle sizes below 150 μm. Four types of belite sulphoaluminate (CSA) cement clinkers, each with varying amounts of BOF slag, were sintered at 1300°C for 30 minutes.
7.	Zingg et al., (2016)[170]	The paper compares high performance concrete (HPC) and low performance concrete (LPC) in triaxial tests, highlighting HPC's reduced capillary porosity and increased compressive strength due to silica fumes and a lower water/cement ratio. LPC, with higher macroscopic porosity from an air-entraining agent, shows lower strength and higher porosity compared to ordinary concrete (OC) under high confinement pressures.
8.	Eskandari-Naddaf and Azimi-Pour, (2018)[162]	A range of dry pressed concrete (DPC) samples was prepared using ordinary Portland cement type II, with strength grades of 32.5, 42.5, and 52.5 MPa.
9.	Sumarni and Wijanarko, (2018)[163]	The mixture includes cement, sand, water, rice straws, and glue. Rice straws are incorporated as fillers by pressing them into bales and then adding them to the concrete brick mould along with the mortar.
10.	Wu, Khayat and Shi, (2019)[171]	The materials utilized consist of Portland cement, silica fume (ranging from 0% to 25%), and straight brass-coated steel fibres with a diameter of 0.2 mm and a length of 13 mm.
11.	Goglio et al., (2021)[172]	In both cold sintering and hydrothermal sintering, a solvent is added to the powder, which is then blended using traditional powder processing methods (such as mortar and pestle, cryomilling, or ball milling) or through a vapor transport process before the sintering process begins.
12.	Zahabi, Said and Memari, (2021)[173]	The primary starting materials were ground and precipitate calcium carbonates (GCC and PCC). Ordinary Portland cement (OPC) and zinc oxide were also examined for comparison purposes.

Table 2.2: Materials used for making Alkali Activated Concrete

Sl. No.	Researchers	Materials Used
1.	Ranjbar et al., (2017)[164]	A low calcium (class F) fly ash is activated with a sodium silicate and sodium hydroxide mixture in a 2.5:1.0 mass ratio. The sodium silicate, in liquid form at 20°C with a density of 1.5 g/mL, has a SiO_2/Na_2O mass ratio of 2.5.
2.	Posi et al., (2017)[174]	The recycled lightweight concrete aggregate (RLCA) was crushed and sorted into coarse aggregate (CA), medium aggregate (MA), and fine aggregate (FA). To lower the weight of the concrete block, a mix with a CA:MA ratio of 30:30:40 by weight was used. The lightweight geopolymer concrete block was made from lignite fly ash, NaOH, Na_2SiO_3, RLCA, and Portland cement (PC).
3.	Wang et al., (2019)[175]	Metakaolin (MK) and fly ash (FA) were used in this study. The alkaline activator, with a modulus of 1.0 (SiO_2/Na_2O ratio = 1.0) and a concentration of 42.5 wt.% (mass fraction of Na_2O + SiO_2 in the solution), was prepared by combining a commercial water glass (containing 12.4 wt.% Na_2O, 32.1 wt.% SiO_2, and 55.5 wt.% H_2O) with a 14 mol/L NaOH solution.
4.	Carvelli et al., (2020)[176]	Stone wool (SW) served as the aluminosilicate precursor. Polyvinyl Alcohol (PVA) fibres were incorporated, and a 5 M sodium hydroxide (NaOH) solution was prepared by dissolving NaOH pellets (from VWR Finland) in deionized water for 10 minutes. The solution was then cooled to room temperature in a sealed plastic bottle and allowed to sit for at least 24 hours before use.
5.	Nguyen et al., (2020)[177]	Solid wool (SW), a byproduct from building insulation, and PVA fibres were used for reinforcement. An alkaline solution was made by weighing NaOH pellets. A 5 M NaOH solution was prepared based on preliminary experiments, aiming for a 28 days compressive strength of 35–40 MPa .
6.	Ranjbar et al., (2020)[178]	Volcanic ash, liquid sodium silicate (containing 30% SiO_2, 12% Na_2O, and 58% H_2O), and 8 M sodium hydroxide were combined in a mass ratio of 2.5:1.0.
7.	Nishikawa, Yamaguchi, et al., (2022)[179]	This study explores how adding silica fume affects the densification and properties of geopolymer products using the warm press method. Geopolymer products, initially hardened by slurry curing with fly ash and sodium hydroxide, were ground into fine particles. Silica fume was then mixed with these particles, and the mixtures were pressed in a steel mould under 240 MPa pressure. The temperature during pressing was gradually increased from 80 to 180°C.

8.	Prasanphan et al., (2020)[180]	The research paper examines the creation of sintered alkali-activated concrete using calcined kaolin processing waste, combined with NaOH flakes and Na_2SiO_3 solution (31.25% SiO_2 ,14.25% Na_2O, and 54.5% H_2O by weight). The geopolymerisation process, involving these materials, results in the formation of geopolymeric gel, which significantly impacts the material's mechanical properties and microstructure.
9.	Shee Ween et al., (2020)[181]	Class F fly ash was activated using a blend of sodium hydroxide (NaOH) and sodium silicate (Na_2SiO_3) solution. The sodium silicate solution had a chemical composition of 30.1% SiO_2, 9.4% Na_2O, and 60.5% H_2O, with a SiO_2/Na_2O ratio of 3.20. A 10 M NaOH solution was prepared by dissolving NaOH pellets in distilled water 24 hours before use.
10.	Nishikawa, Hashimoto, et al., (2022)[182]	Sodium metasilicate hydrate ($Na_2SiO_3 \cdot nH_2O$) was used instead of the alkaline solution(NaOH). Fly ash: Na_2SiO_3: $Na_2SiO_3 \cdot 9H_2O$ (68: 16: 16 wt.%, respectively)
11.	Cao et al., (2023)[166]	Fly-ash-based strain-hardening geopolymer composite (SHGC) plates were manufactured by hot-pressing on a plate vulcanizing press machine.

2.2. Sintering Process

In Table 2.3, the sintering processes for cement concrete are outlined, showcasing varied methodologies and their outcomes. Researchers like Roy, Gouda, and Bobrowsky (1972, 1973) [160] [167] utilized hot-pressing techniques, achieving high compressive strengths by subjecting cement pastes to elevated pressures and temperatures. Mangialardi (2001) [168] explored the enhanced characteristics of sintered products from fly ash with a preliminary washing treatment, meeting Italian requirements for normal weight aggregates. Xue et al. (2016))[169] investigated the sintering process of CSA clinker, utilizing microscopic and analytical techniques. Table 2.4 details sintering processes for alkali-activated concrete, where researchers employed simultaneous heating and pressing techniques to enhance mechanical properties under relatively low temperatures. For instance, Ranjbar et al. (2017) [164] achieved high compressive strength in geopolymer through hot pressing, and Nguyen et al. (2020) [177] employed fixed pressing forces for moulding. These studies collectively contribute to understanding sintering processes, providing insights into optimizing the mechanical properties of both traditional cement concrete and alkali-activated concrete. Fig. 2.1 shows schematic mechanism of geopolymerisation under hot pressing (Ranjbar et al.) [164]. Fig. 2.2 shows schematic mechanism of geopolymerisation under pressure (Shee-Ween *et al.*) [183].

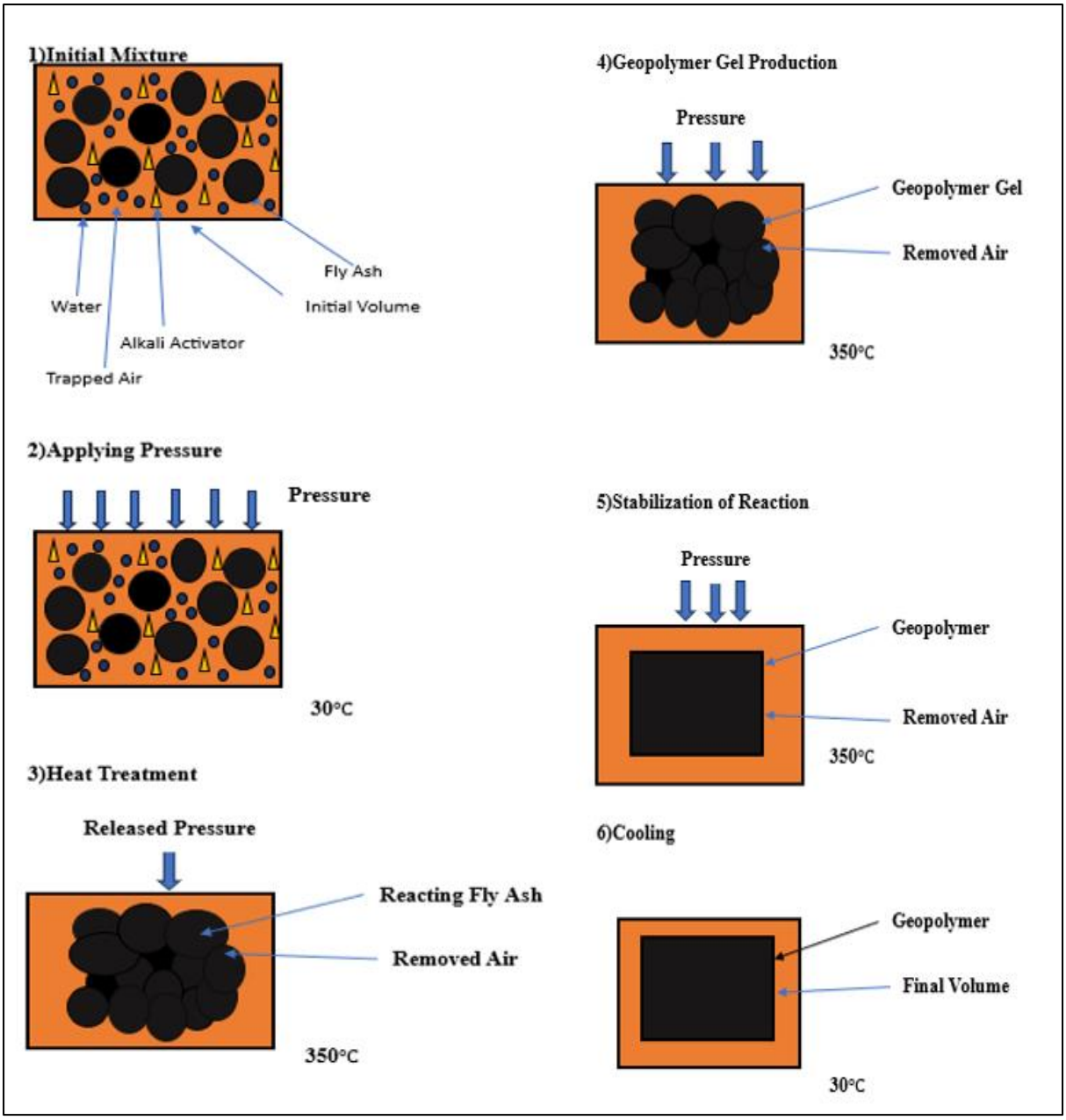

Fig. 2.1: Schematic mechanism of geopolymerisation under hot pressing [164]

Table 2.3: Sintering Process on Cement Concrete

Sl. No.	Researchers	Main Features
1.	Roy, Gouda and Bobrowsky, (1972) [160]	Materials prepared by hot pressing conventional cement pastes, using pressures between 25,000 and 50,000 psi at temperatures close to 150°C, have demonstrated very high strengths with near-zero porosity values. Typical strengths for these hot-pressed samples are 73,900 psi in compression, 59,300 psi in indirect tensile, and 6,320 psi in shear.
2.	Roy and Gouda, (1973)[167]	Materials produced using "hot-pressing" techniques have achieved exceptionally high strengths. Intermediate strength levels have been obtained by applying high pressures at room temperature to Portland cement pastes. When pressing at approximately 250°C and 50,000 psi, compressive strengths can reach up to 95,000 psi, while indirect tensile strengths can attain 9,250 psi.
3.	Mangialardi, (2001)[168]	A preliminary washing treatment of MSW fly ash with water significantly enhanced the chemical and mechanical properties of the sintered products. For all types of fly ash tested, the sintered products met the Italian standards for normal weight aggregates, suitable for use in concretes with specified strengths up to 12 N/mm^2 for cylindrical specimens and 15 N/mm^2 for cubic specimens.
4.	Posi et al., (2013)[161]	In its natural state, diatomite has low reactivity and is a relatively weak material. Calcination removes the combustible components and improves the material's properties.
5.	Wang et al., (2016)[165]	The specimens were subjected to biaxial compressive stress states with stress ratios of 0:1, 0.25:1, 0.5:1, 0.75:1, and 1:1, under both static and varying dynamic loading velocities, with strain rates ranging from 10^{-5} /s to 10^{-2} /s.
6.	Xue et al., (2016)[169]	The sintering process was monitored using microscopy, and its characteristics were analysed with XRD, SEM-EDS, and TAM Air. The results indicated that the degree of sintering of CSA clinker could be predicted by examining its sintering process.
7.	Zingg et al., (2016)[170]	The study explores how the porosity of the cement matrix affects the triaxial behaviour of concrete under high confining pressures. It provides new experimental data on two types of concrete: high-performance concrete (HPC) and low-performance concrete (LPC).
8.	Eskandari-Naddaf and Azimi-Pour, (2018)[162]	The specimen with a water-to-cement ratio of 0.2, a cement content of 400 kg/m^3, and a strength grade of 52.5 MPa exhibited the maximum compressive strength.

9.	Sumarni and Wijanarko, (2018)[163]	Concrete bricks measuring 400×200×100 cm with a 1:7:0.5 cement, sand, and water ratio were sintered at high temperatures to enhance properties. This process achieved a maximum compressive strength of 1.92 MPa, meeting specific gravity and water absorption standards, though results vary with straw volume.
10.	Wu, Khayat and Shi, (2019)[171]	UHPC with 10% to 15% silica fume exhibited the best fibre-matrix bond, as well as superior flexural and tensile properties.
11.	Goglio et al., (2021)[172]	This paper examines two low-temperature sintering processes: hydrothermal sintering, which occurs in closed conditions, and the Cold Sintering Process, which takes place in open conditions.
12.	Zahabi, Said and Memari, (2021)[173]	Compressive strength tests indicated strong performance of OPC mortars with most of the cement replaced by AAC. Scanning electron microscopy revealed effective sintering of calcium carbonate and zinc oxide, achieved through careful selection of solutions.

Table 2.4 :Sintering Process on Alkali Activated Concrete

Sl. No.	Researchers	Main Features
1.	Ranjbar et al., (2017)[164]	This research investigates the use of simultaneous heating and pressing techniques to improve the mechanical properties of fly ash (FA) based geopolymers at relatively low temperatures, aiming for minimal porosity. The findings highlight that the induced pressure is the most influential factor. Specifically, the highest compressive strength of 134 MPa was achieved using hot pressing with a pressure of 41.4 MPa, at a temperature of 35°C, and a duration of 20 minutes.
2.	Posi et al., (2017)[174]	Lightweight geopolymer concrete blocks were produced with 28-day compressive strengths ranging from 2.0 to 14.1 MPa and densities between 1130 and 1370 kg/m³.
3.	Wang et al., (2019)[175]	Inorganic-organic polymer composites (IOPCs) were created by combining geopolymer and epoxy resin through mould pressing. When the epoxy resin content is 4 wt.% and the moulding pressure is 200 MPa, the IOPCs achieve an optimal compressive strength of 116.3 MPa after 3 days of curing.
4.	Carvelli et al., (2020)[176]	This study assesses the impact of the manufacturing process and fibre reinforcement on the low-velocity impact response of newly developed PVA fibre-reinforced alkali-activated stone wool composites. Comparisons were made between specimens reinforced and unreinforced, manufactured through hot-pressing and those cured in an oven. The results showed that the impact

		response of the hot-pressed composite, produced at 120°C for 3 hours, was comparable to that of the oven-cured composite, which was treated at ambient pressure at 60°C for 24 hours.
5.	Nguyen et al., (2020)[177]	Mould with concrete specimen cured between two plates in the machine for 2 to 3 hours at temperatures of 100 or 120°C, using a constant pressing force of 60 kN (approximately 25 MPa), which was controlled automatically.
6.	Ranjbar et al., (2020)[178]	The results show that approximately 65% of the trapped air in the fresh geopolymer matrix is effectively removed with an initial impact pressure. When the pre-compacted matrix undergoes hot-pressing, it becomes further densified by 1–10% due to continuous evaporation of free water and additional compaction.
7.	Nishikawa, Yamaguchi, et al., (2022)[179]	At a warm press temperature of 80°C, the compressive strength of the hardened bodies increased with the amount of added silica fume. Specifically, the compressive strength of a body with 30 wt.% silica fume reached 195 MPa, approximately three times greater than that of a body with 0 wt.% silica fume. The addition of silica fume improved the fine stacking of geopolymer particles during the early stages of warm pressing, leading to objects with tightly packed voids.
8.	Prasanphan et al., (2020)[180]	The study examined the microstructure evolution and mechanical properties of geopolymers made from calcined kaolin processing waste, focusing on the effects of both low and high concentrations of alkali activators.
9.	Shee Ween et al., (2020)[181]	The geopolymer mixtures were formulated with an FA/AA ratio ranging from 4.5 to 7.0 and compacted using a uniaxial hydraulic press. The specimens were then cured at room temperature (30°C) for periods of 7 and 28 days. The highest compressive strength achieved was 78.54 MPa.
10.	Nishikawa, Hashimoto, et al., (2022)[182]	The highest compressive strength was achieved by hardening the material under a uniaxial pressure of 100 MPa at 130°C for just 10 minutes.
11.	Cao et al., (2023)[166]	The results indicated that the load-carrying capacity increased with temperature, pressure, and age, while ductility decreased slightly. At 1 day and 7 days, the specimens achieved 66% and 89% of the load-carrying capacity observed at 28 days, respectively.

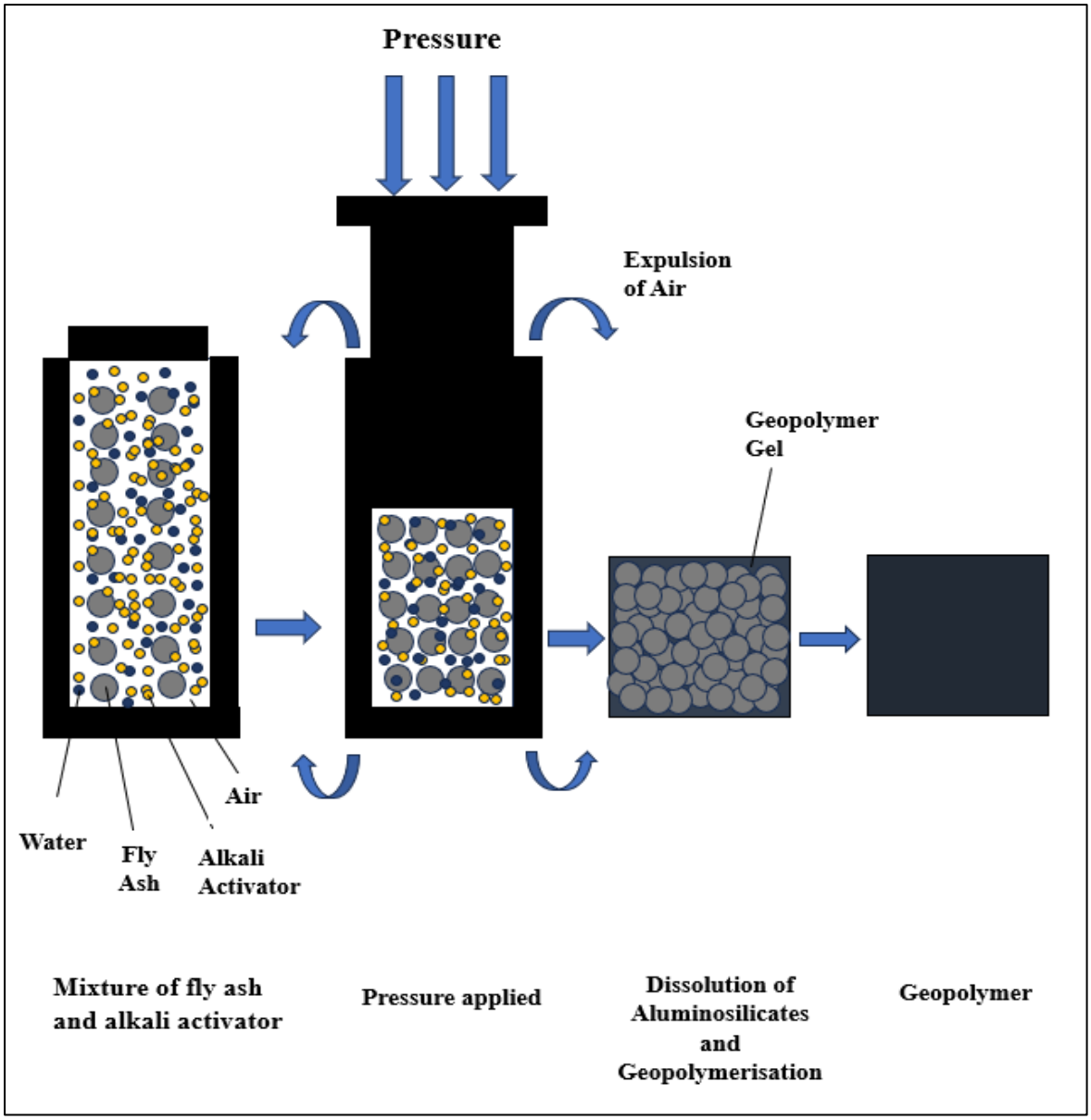

Fig. 2.2: Schematic mechanism of geopolymerisation under pressure [183]

2.3. Improvements due to Sintering Process

Tables 2.5 and 2.6 present the improvements observed in cement concrete and alkali-activated concrete, respectively, resulting from the sintering process. In cement concrete (Table 2.5), researchers like Roy, Gouda, and Bobrowsky (1972, 1973) achieved impressive strengths through hot pressing, showcasing dense microstructures and dimensional stability. Mangialardi (2001) highlighted the significance of washing MSW fly ash for effective sintering, and Posi et al. (2013) demonstrated the stability of coarse aggregate at high temperatures, contributing to lightweight concrete strength. Wu, Khayat, and Shi (2019) discussed the impact of silica

fume on HRWR demand in UHPC. In alkali-activated concrete (Table 2.6), Ranjbar et al. (2017) emphasized the role of hot pressing in developing a more robust geopolymer matrix, leading to higher compressive strength. Fibre reinforcement, as studied by Carvelli et al. (2020) and Nguyen et al. (2020), significantly enhanced impact resistance and mechanical performance. Nishikawa, Yamaguchi, et al. (2022) demonstrated the positive influence of added silica fume on geopolymer particle stacking. Prasanphan et al. (2020) reported higher compressive strength in pressed geopolymer compared to cast geopolymer. Collectively, these studies highlight the diverse improvements in concrete properties achieved through sintering processes, informing the optimization of both traditional and alkali-activated concrete for enhanced performance and durability.

Table 2.5: Improvements due to Sintering Process for Cement Concrete

Sl. No.	Researchers	Main Features
1.	Roy, Gouda and Bobrowsky, (1972) [160]	Specimens prepared under high pressure at 100,000 psi, without elevated temperatures, achieved strengths of 46,100 psi in compression, 4,020 psi in indirect tensile, and 8,400 psi in shear. Scanning electron microscopy revealed very dense microstructures, and exhibited dimensional stability.
2.	Roy and Gouda, (1973)[167]	The hot-pressed materials maintain volume stability when immersed in water. Their microstructures are highly compact, featuring a dense intergrowth of hydrated cement "gel" surrounding residual unhydrated cement grain cores. The lowest porosity recorded for these materials was approximately 1.8%, representing the closest approach to zero porosity.
3.	Mangialardi, (2001)[168]	The sintering process of untreated MSW fly ashes was found to be unsuitable for producing sintered products for construction use due to their unfavourable chemical properties, including high levels of sulphate, chloride, and vitrifying oxides. However, for washed MSW fly ash, the optimal conditions for manufacturing sintered products were identified as a compact pressure of 28 N/mm² with 1140°C temperature for 60 minutes.
4.	Posi et al., (2013)[161]	At 1000°C, the coarse aggregate remained stable and strong, enhancing the strength of the pressed lightweight concrete. At 600°C, the fine diatomite aggregate exhibited reactivity giving us calcined diatomite as an appropriate lightweight aggregate for producing pressed lightweight concrete blocks.
5.	Wang et al., (2016)[165]	The ultimate strengths of both dry and saturated concretes were observed to increase with higher strain rates. Additionally, the

		damage patterns and ultimate strengths are closely linked to the level of lateral pressure applied to the specimen.
6.	Xue et al., (2016)[169]	BOF slag enhances the melting properties of CSA clinkers due to its content of iron oxide, manganese oxide, and magnesium oxide. However, expansion was observed when the temperature reached 420°C, attributed to a combination of factors, including the volatilization of CO_2 from the decomposition of $MgCO_3$ and the thermal expansion of the raw materials .
7.	Zingg et al., (2016)[170]	At high confining pressure the influence of the cement matrix strength—primarily related to its porosity—diminishes. In such conditions, the behaviour of concrete is primarily determined by the granular skeleton, even when capillary porosity is low or entrapped air porosity is high.
8.	Eskandari-Naddaf and Azimi-Pour, (2018)[162]	Porosity affects the durability of curb constructions, while compressive strength and flexural strength are the factors that influence their mechanical properties.
9.	Sumarni and Wijanarko, (2018)[163]	The results indicate that the straw concrete bricks achieved a maximum compressive strength of 1.92 MPa, a specific gravity of 1,702 kg/m³, and a water absorption rate of 3.9%.
10.	Wu, Khayat and Shi, (2019)[171]	The demand for HRWR (High Range Water Reducer) in both the non-fibrous matrix and UHPC initially decreased as the silica fume content increased, but then rose with further additions of silica fume.
11.	(Goglio et al., 2021)[172]	This technique allows for the fabrication of ceramics and ceramics-based composites with advanced properties.
12.	(Zahabi, Said and Memari,2021)[173]	The porosity of sintered samples, as measured by nitrogen adsorption-desorption, showed significant improvement underscoring the potential of cold sintering as a viable alternative for producing conventional precast construction materials.

Table 2.6: Improvements due to Sintering Process for Alkali Activated Concrete

Sl. No.	**Researchers**	**Main Features**
1.	Ranjbar et al., (2017)[164]	The microstructure of the hot-pressed specimens exhibited a more advanced geopolymer matrix compared to conventional methods, resulting in significantly higher compressive strength achieved in a much shorter time. The enhanced mechanical properties are largely due to the material's dense structure and the increased production of geopolymer gel during the hot pressing process.

2.	Posi et al., (2017)[174]	The degree of geopolymerisation improves as the curing temperature rises from 25°C to 90°C, leading to a corresponding increase in compressive strength.
3.	Wang et al., (2019)[175]	The porosity of IOPCs is 22.48%. As the epoxy resin content increases from 0 to 8 wt.%, the porosity gradually rises, while the pore size distribution initially decreases before increasing again.
4.	Carvelli et al., (2020)[176]	Fiber reinforcement and hot-pressing substantially enhances the impact resistance of composites, resulting in an approximately 50% increase in peak load and a 40% reduction in penetration compared to unreinforced materials.
5.	Nguyen et al., (2020)[177]	PVA fibres significantly improved the mechanical performance exhibiting less deflection and increased compressive strength. The hot-pressed PVA fibre-reinforced cementitious composite, produced at 120°C for 2 hours, emerged as the optimal composition.
6.	Ranjbar et al., (2020)[178]	This process not only decreases the size and volume of porosity but also transforms the continuous pore network into a closed structure enhancing geopolymer gel formation and accelerates polycondensation, resulting in relatively high mechanical strength, reaching up to 160 MPa.
7.	Nishikawa, Yamaguchi, et al., (2022)[179]	The addition of silica fume enhanced the fine stacking of initial geopolymer particles during the early stages of warm pressing, facilitating the formation of objects with tightly packed voids between the particles. However, when subjected to heat treatment at a warm press temperature of 180°C, the compressive strength of the hardened pastes containing 30 wt.% silica fume decreased compared to those with 0, 10, and 20 wt.% silica fume.
8.	Prasanphan et al., (2020)[180]	The compressive strength of pressed geopolymer was about 24.39% greater than that of normal cast geopolymer. The highest compressive strength recorded for pressed geopolymer was 27.74 MPa, while for normal cast geopolymer, it was 22.30 MPa.
9.	Shee Ween et al., (2020)[181]	The pressed geopolymer with an FA/AA ratio of 5.5 exhibited the lowest levels of porosity and water absorption. Additionally, SEM micrographs confirmed that this ratio produced a well-compacted microstructure.
10.	Nishikawa, Hashimoto, et al., (2022)[182]	Released free water from $Na_2SiO_3 \cdot 9H_2O$ played a key role in promoting the densification and the geopolymerisation.
11.	Cao et al., (2023)[166]	The plates reinforced with 1.5% by volume fibre gave performance comparable to that for 2%. The plates with oiled polyvinyl alcohol (PVA) fibres are around 20% higher than those with non-oiled PVA fibres in maximum load and deflection under flexure.

2.4. Sintering Effect of Cement Concrete

Roy, Gouda, and Bobrowsky (1972) [160] conducted research on hot pressing cement pastes at high pressures and temperatures, achieving very high strengths with low porosity. Roy and Gouda (1973) [167] also worked on hot-pressing techniques for cement pastes, obtaining unusually high strengths and low porosity. Mangialardi (2001) [168] studied fly ash from incineration plants, finding that sintering improved its characteristics for use in concrete. Posi et al. (2013) [161] researched the use of diatomite in lightweight concrete, highlighting the importance of calcination for improving its properties. Wang et al. (2016) [165] conducted experiments on concrete cubes under different loading conditions and found that the ultimate strength increased with higher strain rates. Xue et al. (2016) [169] examined the sintering of belite sulphoaluminate cement clinkers with various additives, revealing the impact of temperature on sintering and expansion issues. Zingg et al. (2016) [170] investigated the influence of cement matrix porosity on concrete behaviour under high confining pressures, finding that granular skeleton played a significant role. Eskandari-Naddaf and Azimi-Pour (2018) [162] prepared dry pressed concrete samples and showed that porosity influenced durability, while compressive and flexural strength affected mechanical properties. Sumarni and Wijanarko (2018) [163] used rice straws as concrete brick fillers and reported their compressive strength and water absorption properties. Wu, Khayat, and Shi (2019) [171] researched ultra-high-performance concrete (UHPC) with silica fume and steel fibres, indicating that 10-15% silica fume content improved various properties. Goglio et al. (2021) [172] discussed cold sintering and hydrothermal sintering, low-temperature processes for ceramics and composites fabrication with cost-efficiency and low environmental impact. Zahabi, Said, and Memari (2021) [173] explored the use of calcium carbonates and zinc oxide in cement mortars, achieving promising results and improved porosity through cold sintering. Fig. 2.3 shows comparison of compressive strength (MPa) for sintered CC.

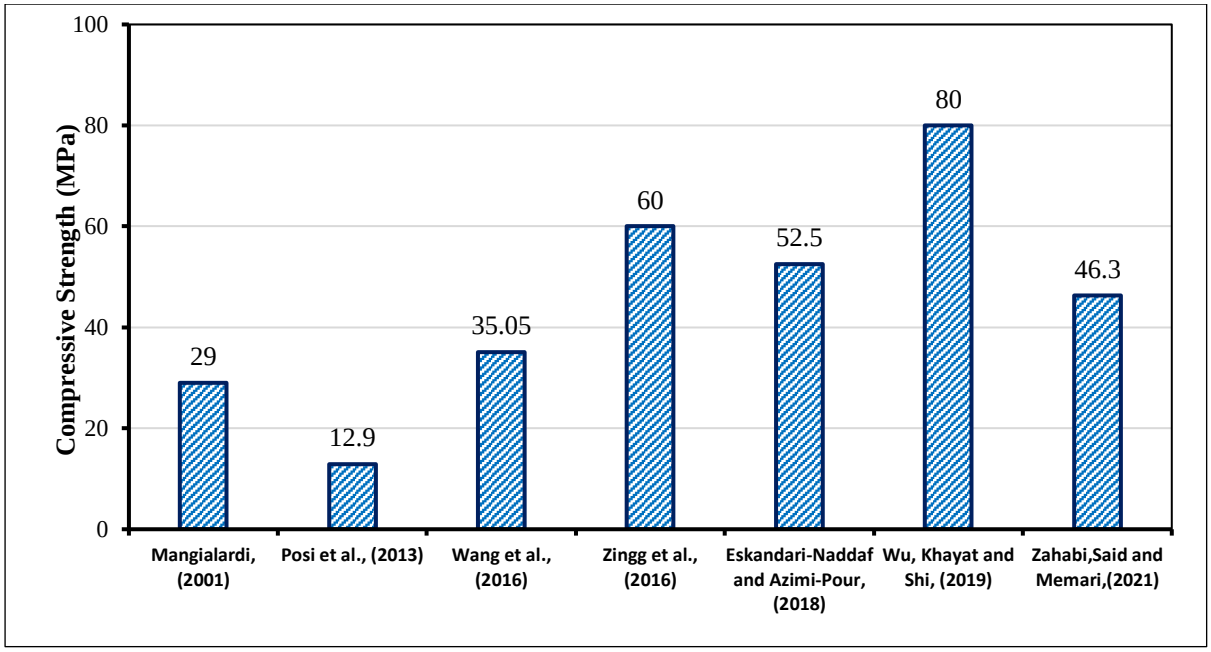

Fig. 2.3: Comparison of Compressive Strength (MPa) for Sintered Cement Concrete

2.5. Sintering Effect of Alkali Activated Concrete

Ranjbar et al. (2017) [164] used hot pressing to enhance the mechanical properties of fly ash-based alkali activated, achieving higher compressive strength through a denser structure. Posi et al. (2017) [174] produced lightweight alkali activated concrete blocks with improved compressive strength by increasing the curing temperature. Wang et al. (2019) [175] created inorganic-organic polymer composites (IOPCs) with higher compressive strength by optimizing epoxy resin content and moulding pressure. Carvelli et al. (2020) [176]found that fibre reinforcement improved impact resistance in PVA fibre-reinforced alkali-activated stone wool composites, both in hot-pressed and oven-cured specimens. Nguyen et al. (2020) [177] demonstrated that PVA fibre reinforcement in hot-pressed cementitious composites improved mechanical performance and reduced CO_2 emissions. Ranjbar et al. (2020) achieved higher mechanical strength through hot pressing of alkali activated, reducing porosity and promoting alkali activated gel formation. Nishikawa, Yamaguchi, et al. (2022) [179]showed that adding silica fume improved compressive strength in alkali activated, especially at lower warm press temperatures. Prasanphan et al. (2020) [180] reported higher compressive strength in pressed alkali activated compared to cast alkali activated using calcined kaolin waste-based alkali activated. Shee Ween et al. (2020) [181] attained high compressive strength with pressed alkali activated, showing lower porosity, especially at specific fly ash/alkali activator ratios. Nishikawa, Hashimoto, et al. (2022) [182] used sodium metasilicate hydrate to achieve high compressive strength through densification. Cao et al. (2023) [166] manufactured strain-

hardening alkali activated composite plates, with increased load-carrying capacity through temperature, pressure, and age, and improved performance with oiled PVA fibres. fig. 2.4 showscomparison of compressive strength (MPa) for sintered AAC.

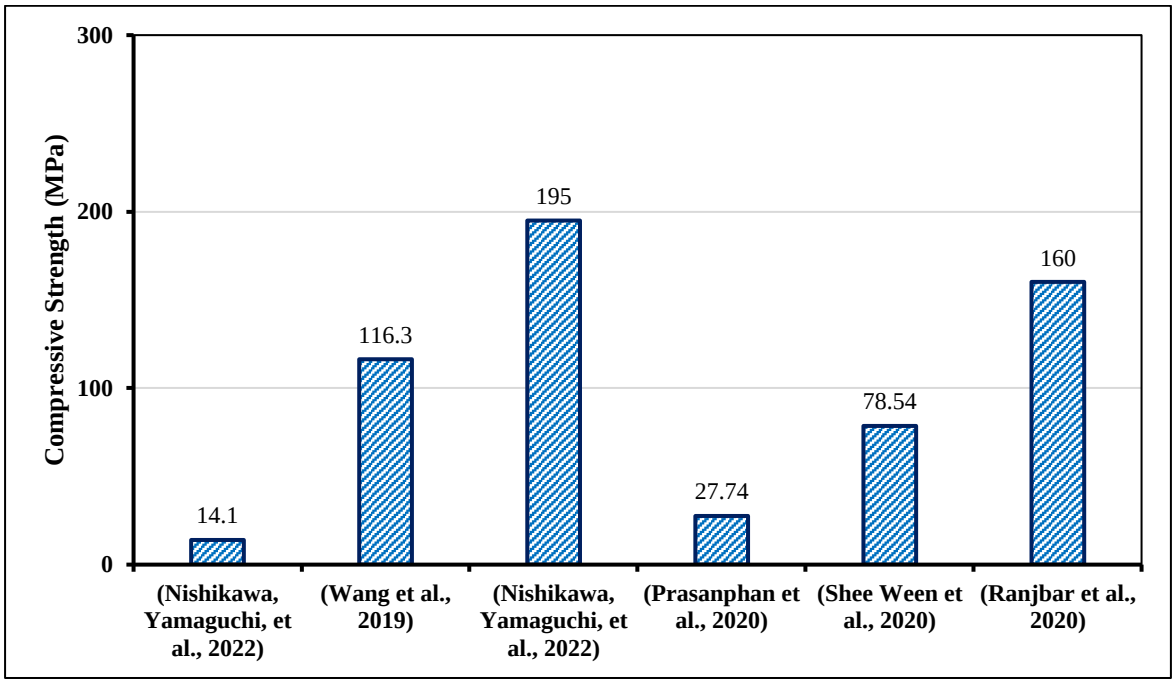

Fig. 2.4 - Comparison of Compressive Strength (MPa) for Sintered Alkali Activated Concrete

2.6. Critical Appraisal of Literature

The literature on sintering processes in traditional CC and AAC reveals several crucial gaps. While studies have addressed short-term improvements in compressive strength, microstructure, and other mechanical properties through sintering, there is a notable lack of comprehensive investigations into long-term durability, structural performance and real-world application. Limited attention has been given to the environmental and economic aspects of sintering processes, hindering a holistic evaluation of ecological footprint, energy consumption, and cost-effectiveness compared to conventional methods. Additionally, there is a need for systematic comparisons across various concrete formulations, and the interaction between sintering conditions and the overall life cycle of concrete remains underexplored. The absence of guidelines, comprehensive reviews, and limited work in the building materials

industry further accentuate the gaps in our understanding. Addressing these issues is crucial for advancing sustainable practices in the construction industry.[184]

The literature reveals several other gaps in the research on sintering processes and alkali-activated concrete (AAC). Although sintering is widely applied in ceramics and metallurgy, its use in the building materials industry remains underexplored. Further studies are needed to investigate the potential of non-ferrous solid waste as a binder in AAC and to analyse the hazards associated with certain AAC components, particularly when scaled up for construction. There is also a need to establish clear relationships between the composition, structure, and strength characteristics of AAC. Additionally, research should focus on making alkali-activated 3D printing a viable construction method and on examining the durability of sintered cement concrete and alkali-activated concrete through tests like rapid chloride penetration and water absorption. The corrosion of reinforcement bars in sintered alkali-activated concrete, as well as the medium to long-term compressive strength and susceptibility to alkali-aggregate and alkali-silica reactions, also require further investigation.

Chapter 3

3. Experimental Program

3.1. Materials

Portland Pozzolana Cement (PPC) with a specific gravity 2.9 was used as binding material in case of CC. River sand with a specific gravity of 2.65 was used as fine aggregate, Crushed stone chips of size 20mm and 10mm with a specific gravity of 2.75 was used as coarse aggregate for preparation of CC specimens. For preparation of AAC, fly ash (FA) of type F and ground granulated blast furnace slag(GGBFS) were used as binding materials, sodium hydroxide(NaOH) pellets and sodium silicate (Na_2SiO_3) were used as activators. Auramix 300, a commercially used superplasticizer manufactured by Fosroc was used in amount of 0.5% w/w of total binding material in preparation of CC and AAC. Potable water was used in preparation of specimens. The properties of binding materials are shown in Table 3.1 and 3.2.

Table 3.1 Physical Properties of Binding Materials

Item	Cement	Fly Ash	GGBFS	Sand(Fine Aggregate)	Stone Chip(Coarse Aggregate)
Specific Gravity	2.9	2.1	2.32	2.65	2.75
Specific Surface(cm^2/gm)	3358	3312	3284		
Colour	Blackish Grey	Blackish Grey	Yellow	Yellow	Yellow

Table 3.2 Chemical Properties of Binding Materials by XRF analysis

Chemicals Present	Fly Ash(%)	GGBFS(%)
CaO	0.88	29.27
SiO_2	55.16	37.23
Al_2O_3	27.18	21.90
MgO	0.76	9.84
Fe_2O_3	5.24	0.34
Na_2O	0.18	0.16
K_2O	1.59	1.33

Sieve analysis is carried out in the laboratory for the determination of zoning of fine aggregate as per Table 9 of IS 383-2016 and coarse aggregate combination of 20mm and 10mm size as per Table 7 of IS 383-2016[185].The results of sieve analysis is represented in fig. 3.1 and fig. 3.2.

As per IS 383-2016, Table 9, the sand belongs to Zone II [185].

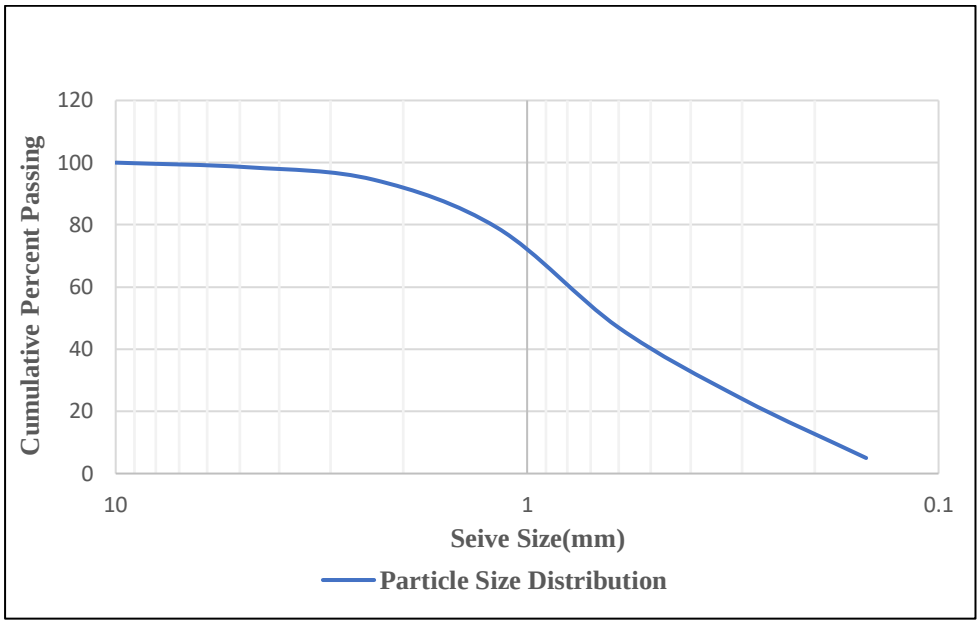

Fig. 3.1 - Sieve Analysis of Fine Aggregates as per IS 383-2016 [185]

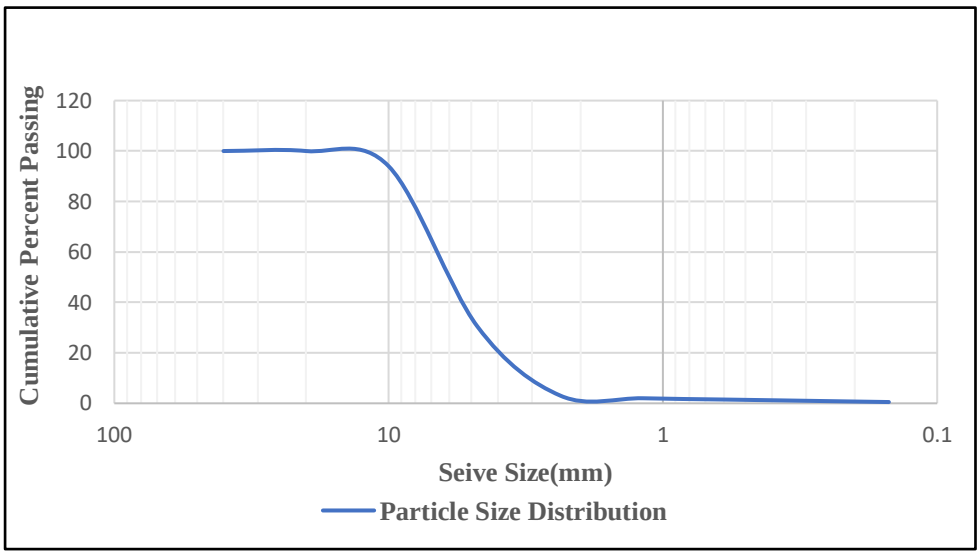

Fig. 3.2 - Sieve Analysis of Coarse Aggregates as per IS 383-2016 [185]

As per IS 383-2016, Table 7(Clause 6.1 & 6.2) these two types of aggregates are used in a mix proportion of 70:30 for 20mm and 10mm stone chips respectively [185].

3.2 Mix Design

Mix designs were made for preparing CC specimen as per IS 10262-2019[186] and AAC as per IS 17452-2020[187].The mix design process is tabulated below. The quantities of materials used for preparation of 1 cubic metre of CC and AAC is tabulated in table 3.3 and 3.4.

Table 3.3 Mix Design for Cement Concrete per cubic metre(cum)

Grade of Concrete	Cement (kg)	Fine Aggregate (kg)	Coarse Aggregate (20mm)(kg)	Coarse Aggregate (10mm) (kg)	Water (kg)	Superplasticizer (ml)(% of Cement)	Water-Cement Ratio
CC-M20	361.5	689.2	796.4	341.3	191.580	0.5	0.530
CC-M25	395.0	661.6	794.2	340.4	191.580	0.5	0.485
CC-M30	445.5	625.4	786.9	337.3	191.580	0.5	0.430

Table 3.4 Mix Design for Alkali Activated Concrete per cubic metre(cum)

Grade of Concrete	Fly Ash (Kg)	GGBFS (Kg)	NaOH(10M) (Kg)	Na_2SiO_3 (Kg)	Fine Aggregate (Kg)	Coarse Aggregate (20mm) (Kg)	Coarse Aggregate (10mm)(Kg)	Added Water (Litre)	Superplasticizer (ml)(% of Binder)	Water-Binder Ratio
AAC-M20	70	280	11.5	127.3	692.1	820.3	351.6	54.2	0.50%	0.45
AAC-M25	75	300	12.3	136.4	677.0	802.4	343.9	48.8	0.50%	0.425
AAC-M30	80	320	13.1	145.5	662.8	785.5	336.7	42.0	0.50%	0.4

3.3 Methodology

3.3.1 Preparation of Specimen

3.3.1.1 Preparation of Cement Concrete Specimen

In order to prepare the test specimens, all raw materials (cement, sand ,stone chips, admixture) were dry mixed for 2- 4 minutes before water was added. The mixing then continued for another 5-8mins. The specimens were prepared depending on the type of test. 3 nos. 100mm cubes were prepared. 3nos. of 100mm diameter &200mm height cylindrical specimens were cast. All the specimens were cast into three equal layers and each layer was compacted for 25 times by the blow of a steel rod of diameter 16mm followed by a vibration on a vibrating table

for 1 minute to remove air bubbles. We will make CC samples of different grades M20, M25, M30. There will be three cases: 1)Normal, 2)Sintering(20kN pressure), 3)Sintering(100℃ for 5mins & 20kN pressure). After 24 hrs the specimens were demoulded. After that, the CC specimens were cured in water reservoir at room temperature of 27℃ for 28 days. The flowchart of preparation of CC is shown in fig. 3.3.

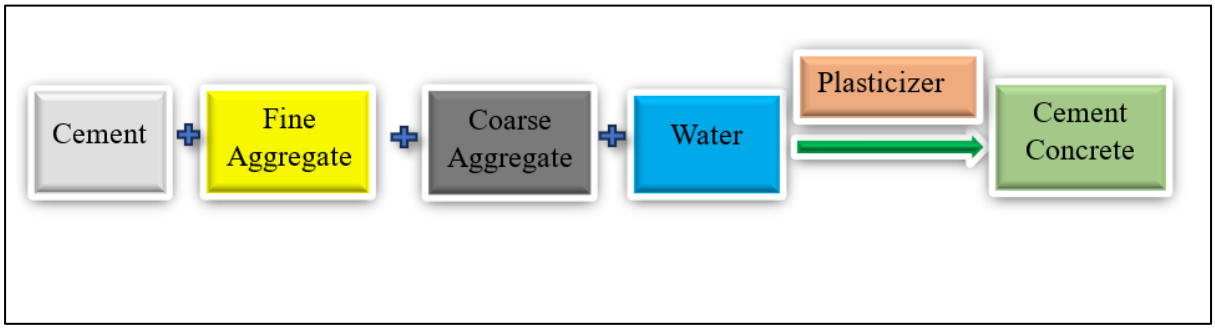

Fig. 3.3 - Flowchart of Preparation of Cement Concrete

3.3.1.2 Preparation of Alkali Activated Concrete Specimen

In order to prepare the test specimens, all raw materials (fly ash, ground granulated blast furnace slag(GGBFS), sand ,stone chips) were dry mixed for 2- 4 minutes before sodium hydroxide (NaOH) solution, sodium silicate (Na_2SiO_3), admixture were added. NaOH pellets had to be put under water 24 hrs before the casting process which then needed to be mixed with Na_2SiO_3 .The mixing then continued for another 5-8mins. The specimens were prepared depending on the type of test. 3 nos. 100mm cubes were prepared. 3nos. of 100mm diameter & 200mm height cylindrical specimens were cast. All the specimens were cast into three equal layers and each layer was compacted for 25 times by the blow of a steel rod of diameter 16mm followed by a vibration on a vibrating table for 1 minute to remove air bubbles. We will make AAC samples of different grades M20, M25, M30. There will be three cases: 1)Normal ,2)Sintering(20kN pressure), 3)Sintering(100℃ for 5mins & 20kN pressure). AAC specimens were put in the furnace along with the mould at 60℃ for 1 day just after casting. AAC specimens were cured at 60℃ in furnace for 2 days(48 hrs) for thermal curing just after casting without demoulding then it was demoulded after 2 days. Then AAC specimens were kept at room temperature of 27℃ for another 26 days. The flowchart of preparation of AAC is shown in fig. 3.4. Materials for making CC and AAC is shown Fig. 3.5. Fig. 3.6 shows flowchart of sintering of CC and AAC. Fig. 3.7 shows Sintering of CC and AAC using (a) pressure ,(b) heat.

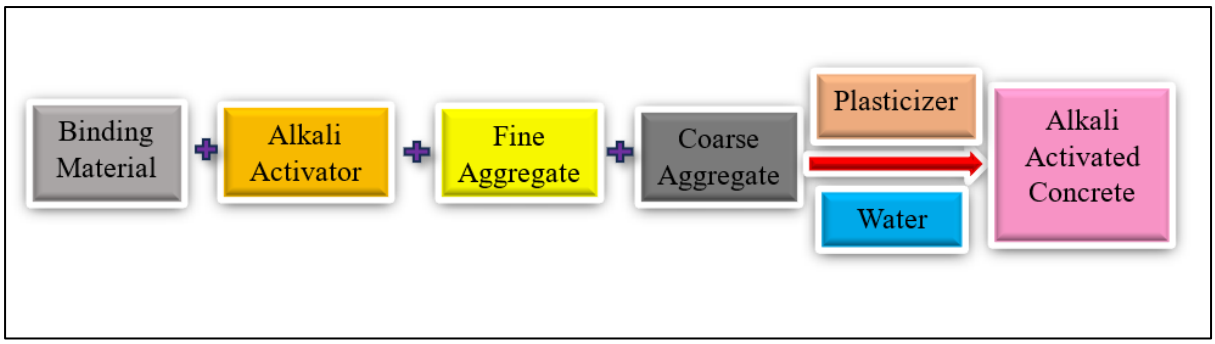

Fig. 3.4 - Flowchart of Preparation of Alkali Activated Concrete

		
Cement	Sand (Fine Aggregate)	Stone Chip (Coarse Aggregate)
		
Superplasticizer	Sodium Hydroxide	Fly Ash

	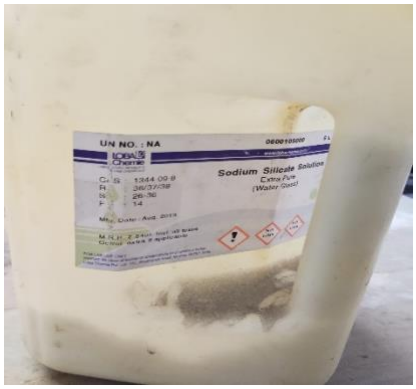	
GGBFS	Sodium Silicate	Furnace

Fig. 3.5 -Materials for making Cement Concrete and Alkali Activated Concrete

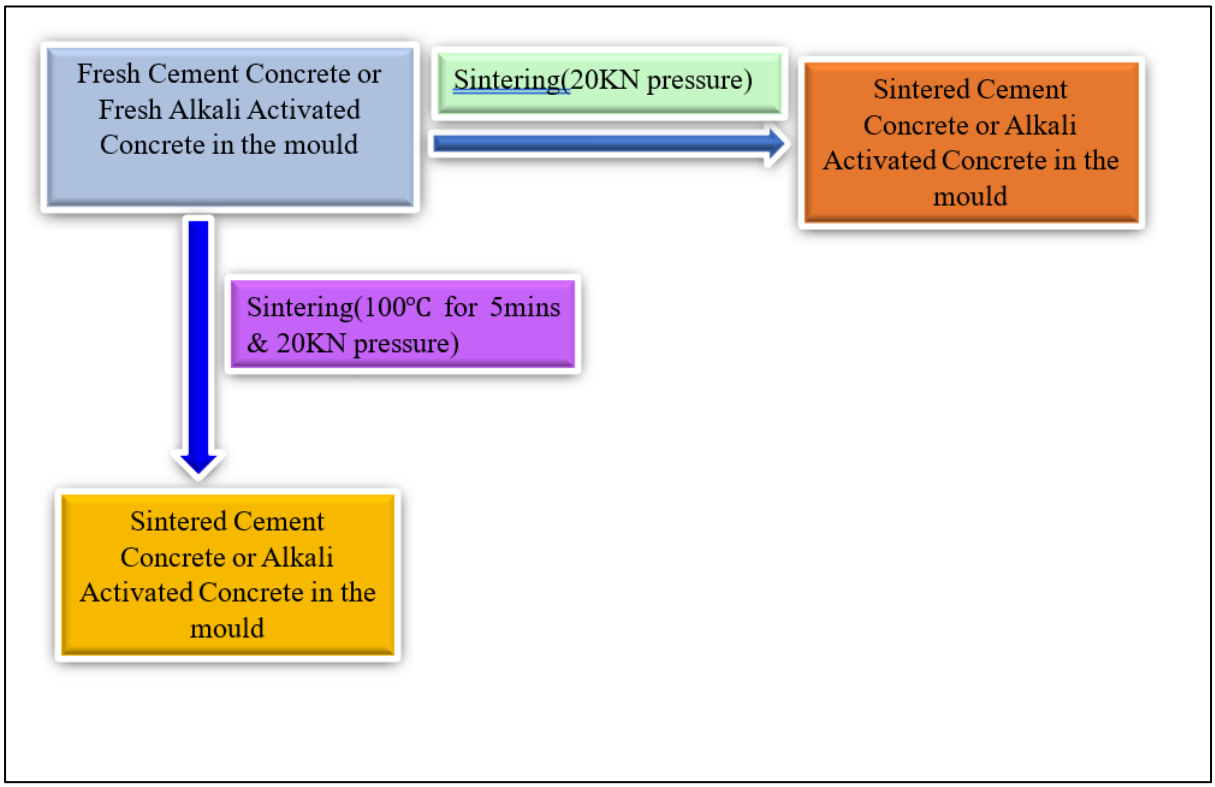

Fig. 3.6 - Flowchart of Sintering of Cement Concrete and Alkali Activated Concrete

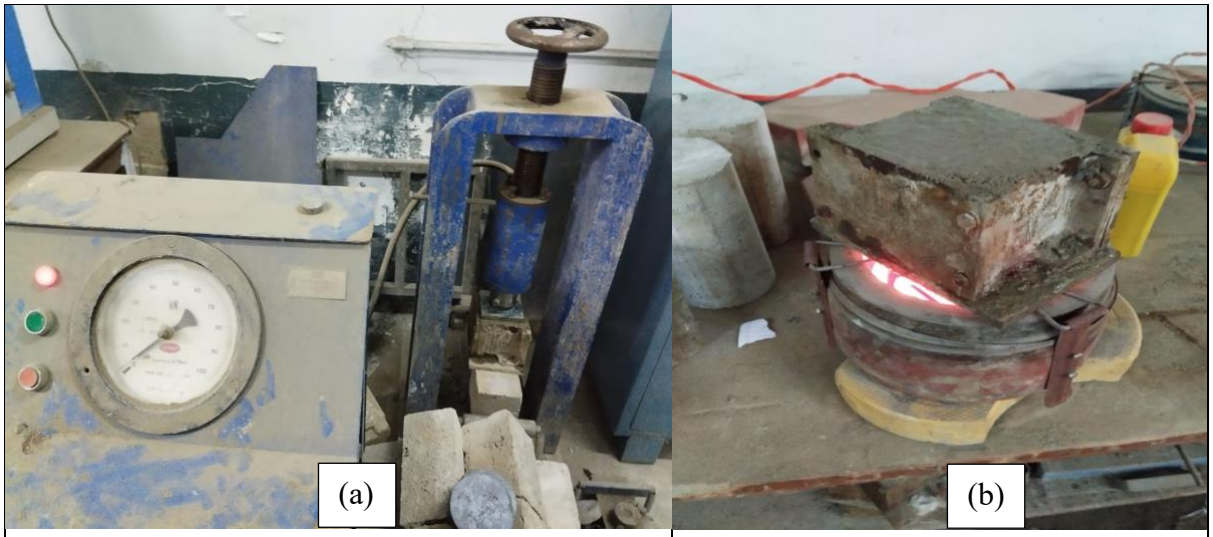

Fig. 3.7 - Sintering of Cement Concrete and Alkali Activated Concrete using (a) pressure (b) heat

3.3.2 Testing Process

At 28 days from the date of casting of specimens several tests were performed in the laboratory, on the specimens and the average value of three specimens was taken as the result.

3.3.2.1 Mechanical Tests

3.3.2.1.1 Compressive Strength Test

Compressive strength in concrete is defined by a characteristic value indicating that no more than 5% of test results should fall below this threshold. This test is crucial in construction to ensure concrete meets safety and durability standards. The test involves placing a specimen in a compression testing machine, which applies a gradual load of 14 N/mm²/min until the specimen fails. The compressive strength is calculated as the maximum load divided by the cross-sectional area, and the final value is the average of three test results, provided individual variations do not exceed ±15% of this average[188]. Fig. 3.8 -(a) shows compressive strength test of a cube specimen.

3.3.2.1.2 Split Tensile Strength Test

The split tensile strength test measures concrete's tensile strength, an important property since concrete is strong in compression but weak in tension. This test uses cylindrical samples. We

had taken samples of 100 mm in diameter and 200 mm in height and placed them horizontally in a compression testing machine. A uniform load of about 2 N/mm²/min is applied until the specimen fails by splitting along its diameter. The maximum load at failure is recorded, and the split tensile strength is calculated with the formula T $=\frac{2P}{\pi DL}$ where P is the maximum load, D is the diameter, and L is the length of the specimen[188]. Fig. 3.8 (b) shows Split tensile strength test of a cylindrical specimen.

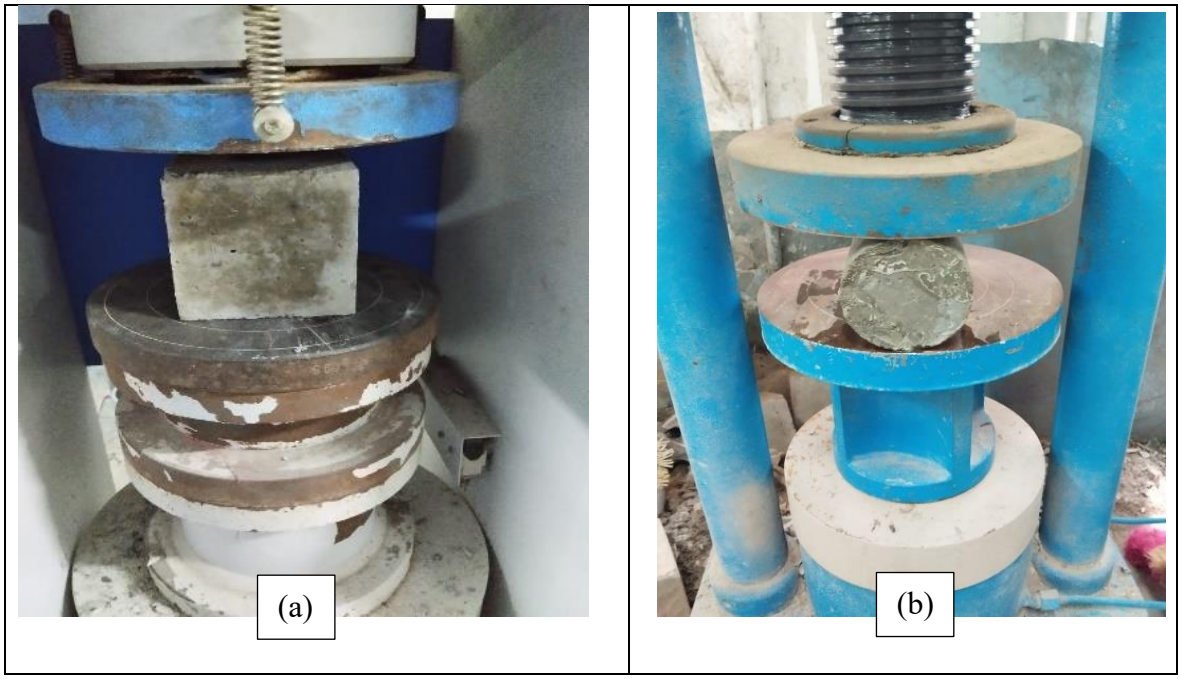

Fig. 3.8 -(a) Compressive strength test of a cube specimen (b) Split tensile strength test of a cylindrical specimen

3.3.2.2 Non Destructive Tests on Concrete Specimens

3.3.2.2.1 Rebound Hammer Test

The Rebound Hammer Test, or Schmidt Hammer Test, is a non-destructive method used to evaluate the surface hardness and indirectly estimate the compressive strength of concrete. Valued for its simplicity and quick results, this test aids in quality control and detecting potential weaknesses in concrete structures without causing damage. Conducted according to Is 516 standard , it involves preparing the concrete surface by ensuring it is smooth, clean, and dry. The hammer is calibrated and then held perpendicular to the surface. After releasing the hammer mass to impact the concrete, the rebound number is read from the hammer's scale.

Multiple readings are taken from various locations to account for variability, and the average is used to estimate compressive strength. The rebound number, which reflects surface hardness, is correlated with compressive strength using established calibration curves, with higher rebound numbers generally indicating higher strength[189]. Fig.- 3.9 (a) shows Rebound hammer .

3.3.2.2.2 Ultrasonic Pulse Velocity (UPV) test

The Ultrasonic Pulse Velocity (UPV) test, as outlined by Indian Standard IS 516, is a non-destructive method for evaluating the quality and consistency of concrete by measuring the time it takes for an ultrasonic pulse to traverse the material. This test helps estimate concrete strength, detect internal flaws, and assess uniformity. To perform the UPV test, essential equipment includes an ultrasonic pulse generator and receiver, transducers to convert signals, a couplant for effective contact, and a timing device. The procedure involves preparing the concrete surface, applying the couplant, and using one of three transducer placement methods: direct, semi-direct, or indirect transmission. The pulse velocity is calculated using the formula $V=\frac{L}{T}$, where V is the pulse velocity in meters per second (m/s), L is the path length in meters (m), and T is the travel time in seconds (s). High pulse velocities indicate good quality concrete with high density and uniformity, while low velocities suggest poor quality with potential issues such as porosity or internal defects. According to IS 516 (Part 5/Sec 1): 2018, concrete is graded based on pulse velocity as follows: Excellent (above 4.40 km/s), Good (3.75 to 4.40 km/s), Doubtful (3.00 to 3.75 km/s), and Poor (below 3.00 km/s). For concrete classified as 'Doubtful,' further testing may be required to ensure quality[190]. Fig.- 3.9 (b), (c) shows UPV test of concrete specimen.

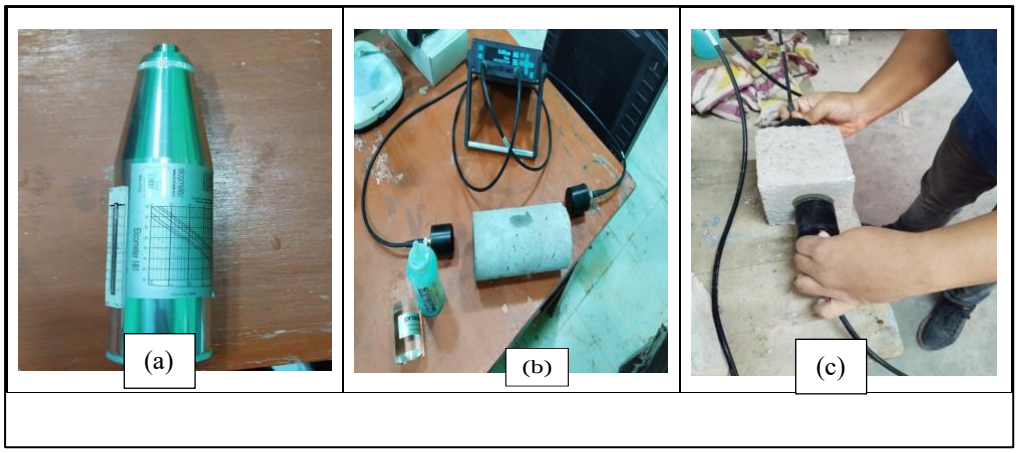

Fig.- 3.9 (a) Rebound hammer (b), (c)UPV test of concrete specimen

3.3.2.3 Durability Tests on Concrete Specimens

3.3.2.3.1 Rate of Absorption of Water (Sorptivity) Test

The sorptivity test is essential for assessing the durability and permeability of concrete by measuring how quickly it absorbs water. According to ASTM C1585, the test involves preparing cylindrical concrete specimens, typically 100 mm in diameter and 30 mm in height, which are first dried at 50 ± 2°C until a constant mass is achieved. After cooling, the specimens are sealed with epoxy paint on their lateral surfaces to ensure that water absorption occurs only through the bottom. The specimens are then placed in a shallow tray with water, maintaining a water level 1 to 3 mm above the supports, and the increase in mass is measured at specific intervals—1, 5, 10, 20, 30, and 60 minutes, and then daily up to 7 days. The cumulative water absorption is calculated and plotted against the square root of time (√t), with the initial slope representing the sorptivity of the concrete. High sorptivity values indicate greater porosity and potential durability issues, such as susceptibility to freeze-thaw cycles and chloride ingress, while low sorptivity values suggest denser, more durable concrete with lower permeability[191]. Fig. 3.10 shows (a)Cutting the specimen (b) Epoxy Paint (c)Sorptivity test setup.

3.3.2.3.2 Rapid Chloride Permeability Test (RCPT)

The Rapid Chloride Permeability Test (RCPT), defined by ASTM C1202, assesses the resistance of concrete to chloride ion penetration, crucial for evaluating the durability of structures exposed to chloride-rich environments like marine structures and pavements. The test measures the electrical charge passed through cylindrical concrete specimens, typically 100 mm in diameter and 50 mm thick, to gauge their permeability. Specimens are saturated in de-aired water, positioned between cells containing a 3% NaCl solution (cathode) and a 0.3N NaOH solution (anode), and sealed to prevent leakage. A constant 60V DC is applied, and the current is recorded at 30-minute intervals over a 6-hour period. The total charge passed is calculated and classified to determine the concrete's chloride ion penetrability: greater than 4000 Coulombs indicates high permeability, 2000-4000 Coulombs moderate, 1000-2000 Coulombs low, 100-1000 Coulombs very low, and less than 100 Coulombs negligible. This test is vital for durability assessment, quality control, and predicting the service life of concrete structures, helping to prevent corrosion and ensure long-term performance[192]. Fig. 3.10

shows (d)Sodium Hydroxide Pellets (e)Sodium Chloride (f)Industrial Grease (g) Rapid Chloride Permeability Test.

3.3.2.4 Microstructural Study using Optical Microscope and Image J Software

To conduct a microstructural study of concrete using an optical microscope and ImageJ software, begin with sample preparation by cutting and polishing the concrete to achieve a smooth surface, then mount it for microscopic analysis. Capture images of the concrete's microstructure at various magnifications using the optical microscope. Import these images into ImageJ software, calibrate the scale, and enhance the images by adjusting contrast and segmenting different components such as aggregates and voids. Measure key parameters, including aggregate size, porosity, and cracks, to analyse the concrete's microstructure. Finally, interpret the results by comparing them with expected outcomes to correlate the microstructural features with the concrete's overall properties. This analysis provides insights into the concrete's quality and performance by linking its microstructure to its functional characteristics[193]. Fig. 3.10 (h) shows Microstructural study of concrete using an optical microscope.

(a)

(b)

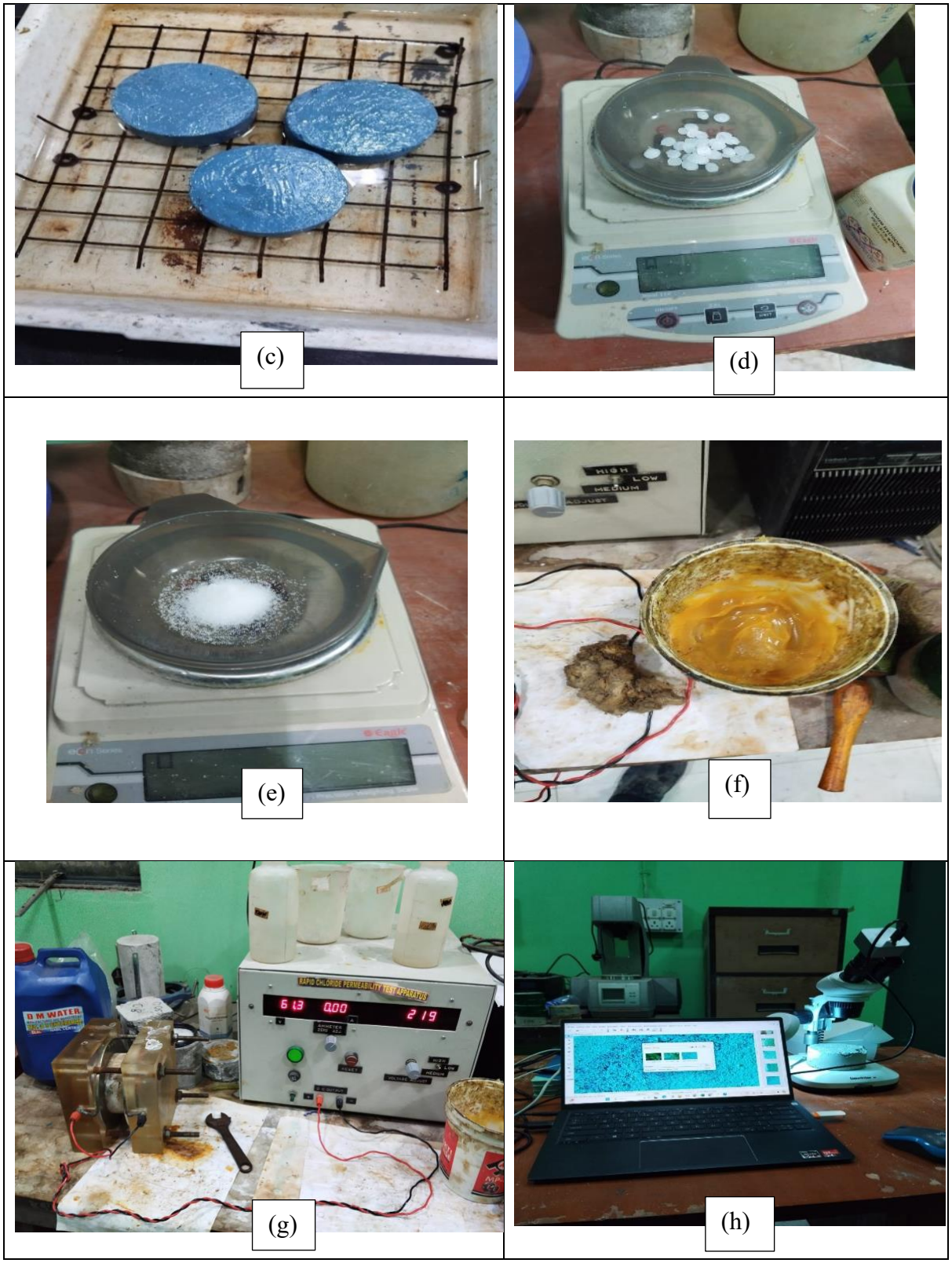

Fig. 3.10 - (a)Cutting the specimen (b) Epoxy Paint (c)Sorptivity test setup(d)Sodium Hydroxide Pellets (e)Sodium Chloride (f)Industrial Grease (g) Rapid Chloride Permeability Test (h)Microstructural study of concrete using an optical microscope.

Chapter 4

4. Results and Discussions

4.1 Compressive Strength Test Results

Compressive Strength Test Results of Various Concrete Specimens with different sintering conditions are tabulated below. '1' refers to Normal condition, '2' refers to Sintering(20kN pressure) and '3' refers to Sintering(100℃ for 5mins & 20kN pressure).

The result highlights the impact of different sintering conditions on the compressive strength of CC and AAC across grades M20, M25, and M30. The area of sintered specimens decreases as length of the specimens decrease. Without sintering, CC and AAC showed compressive strengths ranging from 33 to 42.6 MPa and 32.1 to 42.7 MPa, respectively. When sintered under 20kN pressure, the compressive strengths increased, with CC ranging from 40.7 to 46.8 MPa and AAC from 40.3 to 47 MPa. The most significant improvement was observed under sintering at 100℃ for 5 minutes with 20kN pressure, where CC's compressive strength ranged from 45.3 to 52.7 MPa, and AAC's strength ranged from 45.2 to 54 MPa. This data indicates that sintering, particularly under the third condition, significantly enhances the compressive strength of both CC and AAC. Fig. 4.1 shows comparison of compressive strength of sintered CC and AAC specimens.

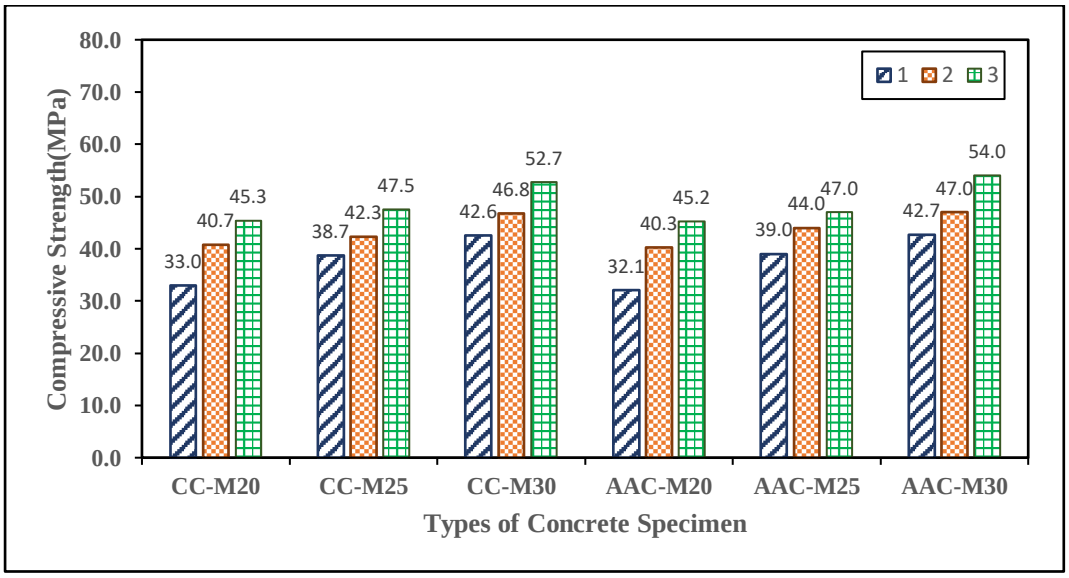

Fig. 4.1 -Comparison of Compressive Strength of Sintered Cement Concrete and Alkali Activated Concrete Specimens

4.2 Split Tensile Strength Test Results

The data illustrates the impact of various sintering conditions on the split tensile strength of CC and AAC for grades M20, M25, and M30. In the case of CC, the M20 grade begins with a split tensile strength of 3.8 MPa without sintering, which increases to 4.5 MPa under 20kN pressure, and further to 5 MPa with additional sintering at 100°C for 5 minutes. The M25 grade shows a similar progression, with strengths of 4.5 MPa, 5.1 MPa, and 5.5 MPa under the respective conditions. The M30 grade achieves 5.2 MPa without sintering, 6.2 MPa under 20kN pressure, and reaches 6.7 MPa with full sintering.

For AAC, the M20 grade's tensile strength starts at 4.1 MPa without sintering, increases to 4.9 MPa under 20kN pressure, and rises to 5.4 MPa with full sintering. The M25 grade follows this pattern, with strengths of 4.8 MPa, 5.5 MPa, and 6 MPa, while the M30 grade improves from 5.6 MPa to 6.5 MPa, and peaks at 7 MPa with full sintering. These results demonstrate that sintering, especially at 100°C for 5 minutes with 20kN pressure, significantly enhances the split tensile strength of both CC and AAC across all grades. Fig. 4.2 shows comparison of split tensile strength of sintered cement concrete and alkali activated concrete specimens.

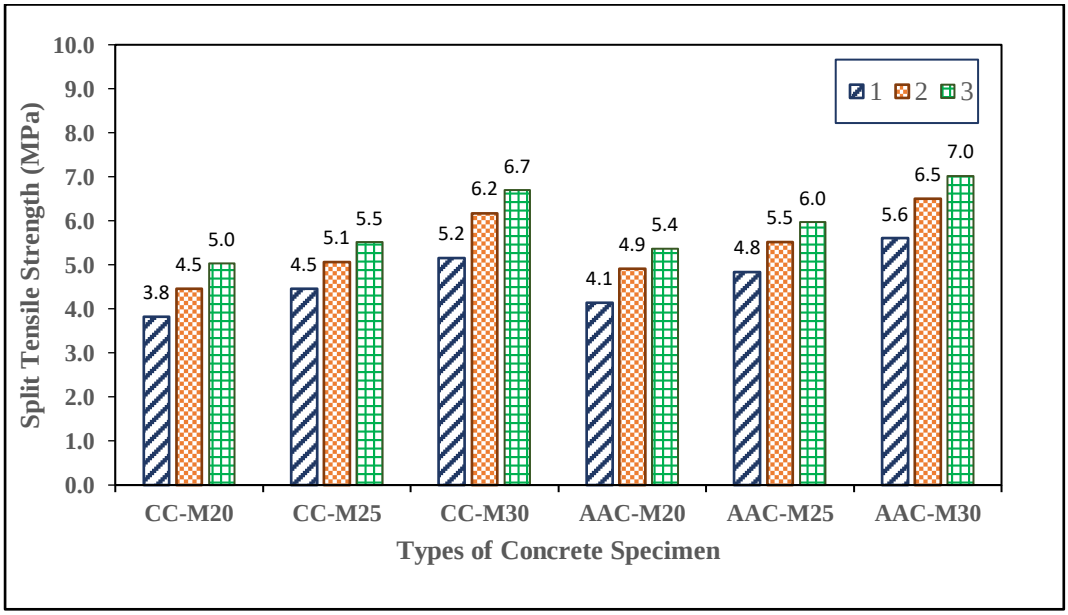

Fig. 4.2 - Comparison of Split Tensile Strength of Sintered Cement Concrete and Alkali Activated Concrete Specimens

Split tensile Strength of AAC is more than CC . Here the split tensile strength of all the specimens(100 mm in diameter and 200 mm in height) will come higher than usual specimens(150 mm in diameter and 300 mm in height) as the dimensions are smaller[194]. Also, we can see with the increase of sintering effort split tensile strength increases of all types and grades of concrete.

4.3 Rebound Hammer Test Results

The data shows that sintering significantly improves the rebound number and cube compressive strength of CC and AAC. For CC, the M20 grade's rebound number increases from 29 to 37 and its compressive strength from 21 MPa to 33 MPa with sintering. The M25 grade progresses from 35 to 41 rebound numbers and from 30 MPa to 38 MPa. The M30 grade improves from 37 to 45 rebound numbers and from 34 MPa to 46 MPa. For AAC, the M20 grade's rebound number rises from 27 to 36, and compressive strength from 20 MPa to 31 MPa. The M25 grade increases from 34 to 40 rebound numbers and from 28 MPa to 37 MPa. The M30 grade sees a rise from 38 to 47 in rebound number and from 34 MPa to 50 MPa in compressive strength with sintering. Fig. 4.3 shows comparison of cube compressive strength from rebound hammer test results of sintered CC and AAC specimens.

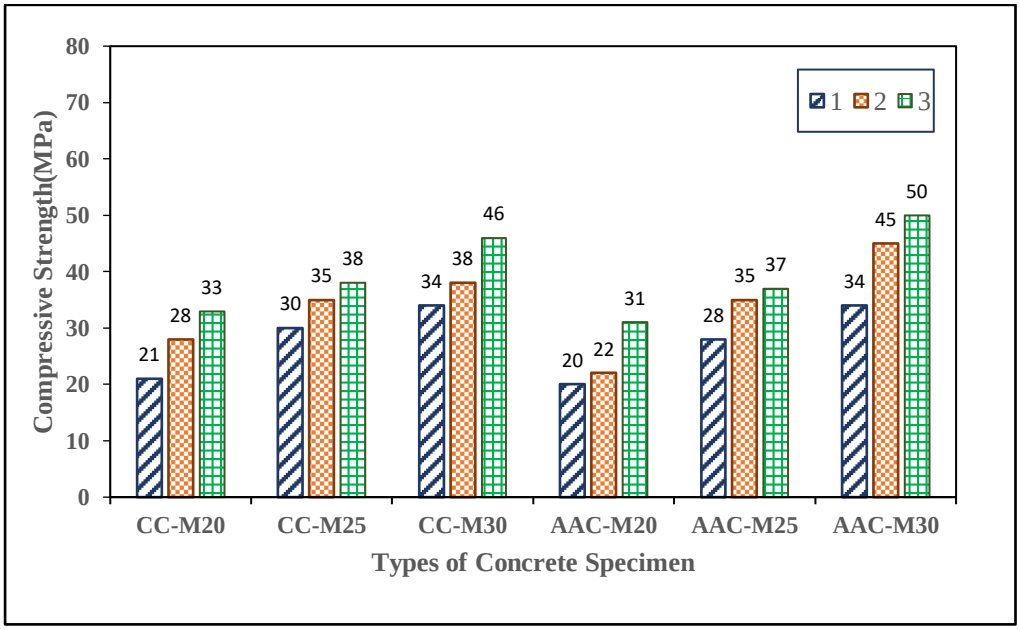

Fig. 4.3 - Comparison of Cube Compressive Strength from Rebound Hammer Test Results of Sintered Cement Concrete and Alkali Activated Concrete Specimens

4.4 Ultrasonic Pulse Velocity (UPV) Test Results

The result highlights how different sintering conditions affect pulse velocity and quality grading for CC and AAC across grades M20, M25, and M30. For CC, pulse velocities improve with enhanced sintering: starting at 3.6 km/s for M20 without sintering, increasing to 3.7 km/s with sintering under 20kN pressure, and reaching 3.9 km/s with full sintering at 100℃ for 5 minutes and 20kN pressure. Similarly, M25 shows an increase from 3.8 km/s without sintering to 4 km/s with 20kN pressure, and up to 4.2 km/s with full sintering. For M30, velocities rise from 3.9 km/s without sintering to 4.2 km/s with 20kN pressure, peaking at 4.4 km/s with full sintering, with all grades rated as "Good."

In AAC, M20's pulse velocity starts at 3.7 km/s, improves to 3.8 km/s with 20kN pressure, and reaches 3.9 km/s with full sintering. The M25 grade increases from 4 km/s to 4.1 km/s, and up to 4.2 km/s with full sintering. For M30, the velocity rises from 4.1 km/s to 4.2 km/s, and peaks at 4.4 km/s with full sintering, with all samples also rated as "Good." This demonstrates that enhanced sintering conditions effectively boost pulse velocity for both types of concrete. Fig. 4.4 shows comparison of ultrasonic pulse velocity test results of sintered cement concrete and alkali activated concrete specimens .

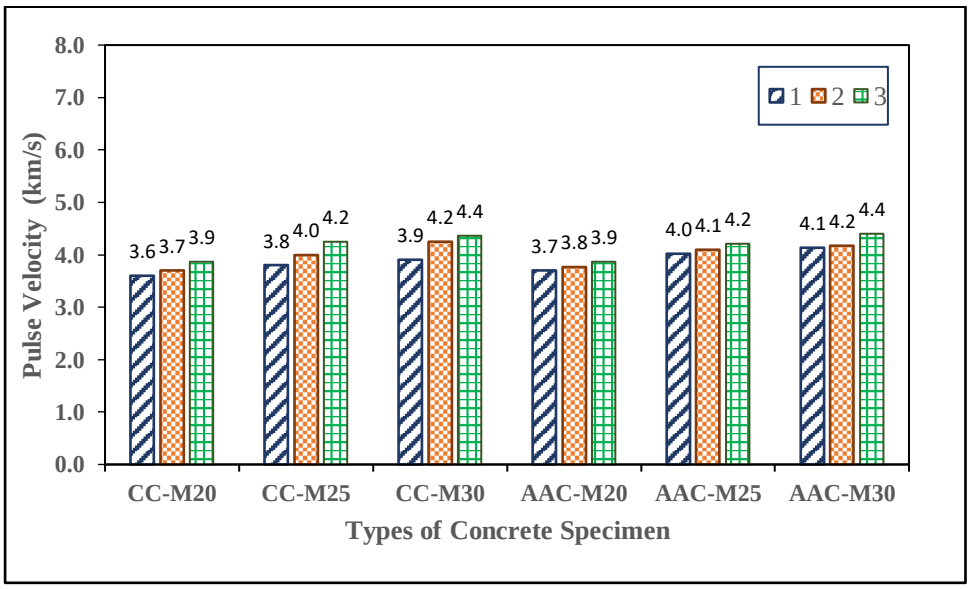

Fig. 4.4 - Comparison of Ultrasonic Pulse Velocity (UPV) Test Results of Sintered Cement Concrete and Alkali Activated Concrete Specimens

4.5 Rate of Absorption of Water (Sorptivity) Test Results

In this study, the relationship between sintering efforts and water absorption in CC and AAC were evaluated through various test samples. It was observed that increasing the sintering effort led to a reduction in water absorption, as evidenced by the mass gain of the concrete samples over time. The initial set of samples, which underwent no sintering, showed a significant increase in mass due to higher water absorption. However, as sintering efforts intensified—both in terms of applied pressure and temperature—the rate of water absorption decreased, resulting in a lesser increase in mass. This indicates that the sintering process enhances the densification of the concrete matrix, thereby reducing its porosity and, consequently, its sorptivity. The enhanced sintering not only improves the mechanical properties of the concrete but also minimizes its susceptibility to moisture penetration, which is critical for the longevity and durability of concrete structures. Fig. 4.5 shows comparison of sorptivity test results of sintered CC specimens.

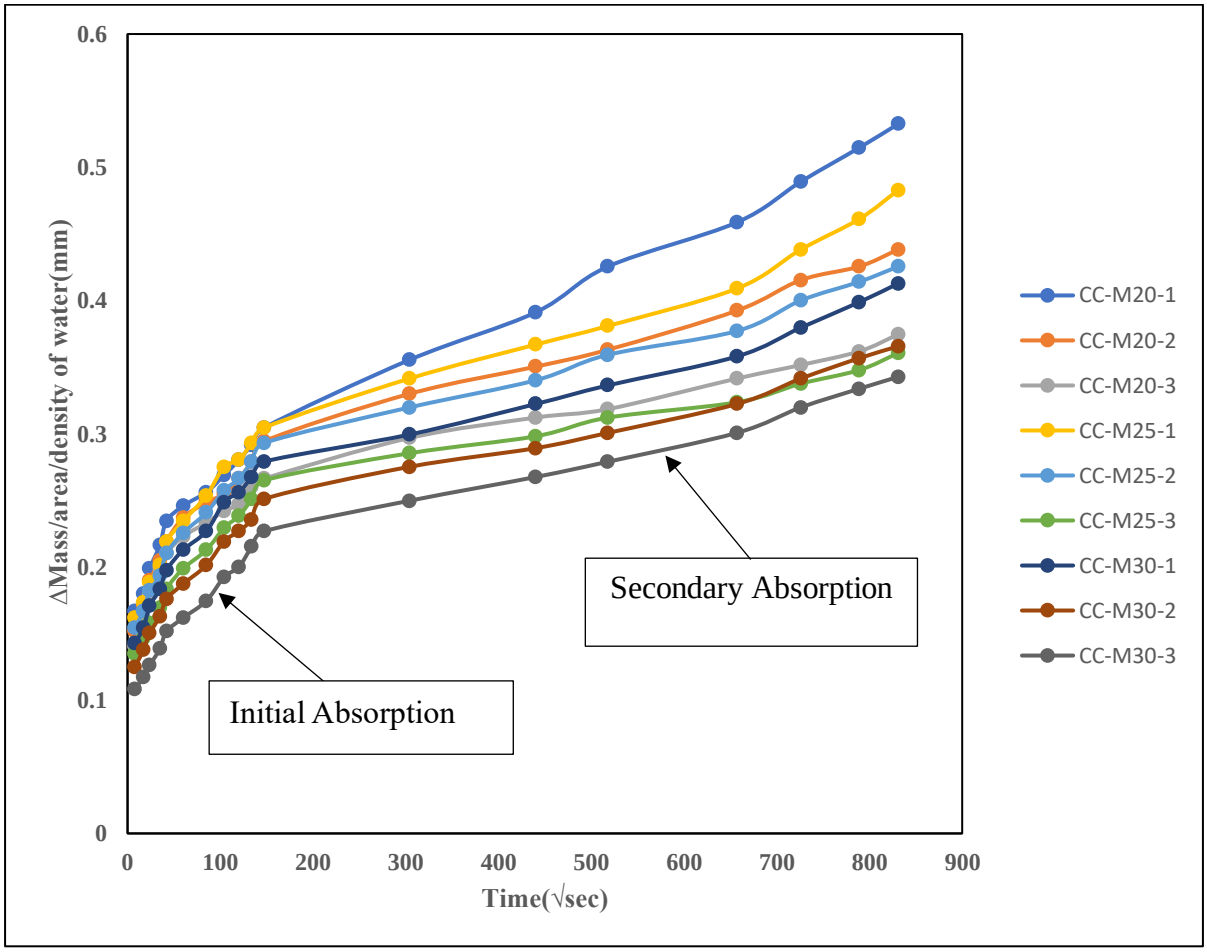

Fig. 4.5- Comparison of Sorptivity Test Results of Sintered Cement Concrete Specimens

The results illustrate a comparison between the sorptivity of AAC and what can be inferred as typical CC in terms of water absorption over time. Sorptivity, which measures the ability of a material to absorb water by capillarity, is a critical parameter for evaluating the durability of concrete, especially its resistance to water ingress. From the data, it is evident that AAC exhibits lower sorptivity compared to what would typically be expected from conventional CC. The reduced sorptivity in AAC is attributed to its denser microstructure and reduced porosity, which result from the alkali activation process. This process enhances the binding of particles within the concrete matrix, leading to a material that is less permeable to water. The data further shows that as the sintering effort increases, the sorptivity of the AAC samples decreases even further. This means that AAC not only starts with a lower sorptivity compared to traditional CC but also has the potential to be further improved by additional densification techniques, such as applying pressure and heat. This enhancement results in AAC becoming even less prone to water absorption, which is crucial for increasing the durability and longevity of concrete structures exposed to moisture. In summary, AAC offers superior resistance to water absorption compared to conventional CC, as evidenced by its lower sorptivity values. The data supports the conclusion that AAC, particularly when subjected to enhanced sintering techniques, is a more durable and water-resistant material. Fig. 4.6 shows comparison of sorptivity test results of sintered AAC specimens.

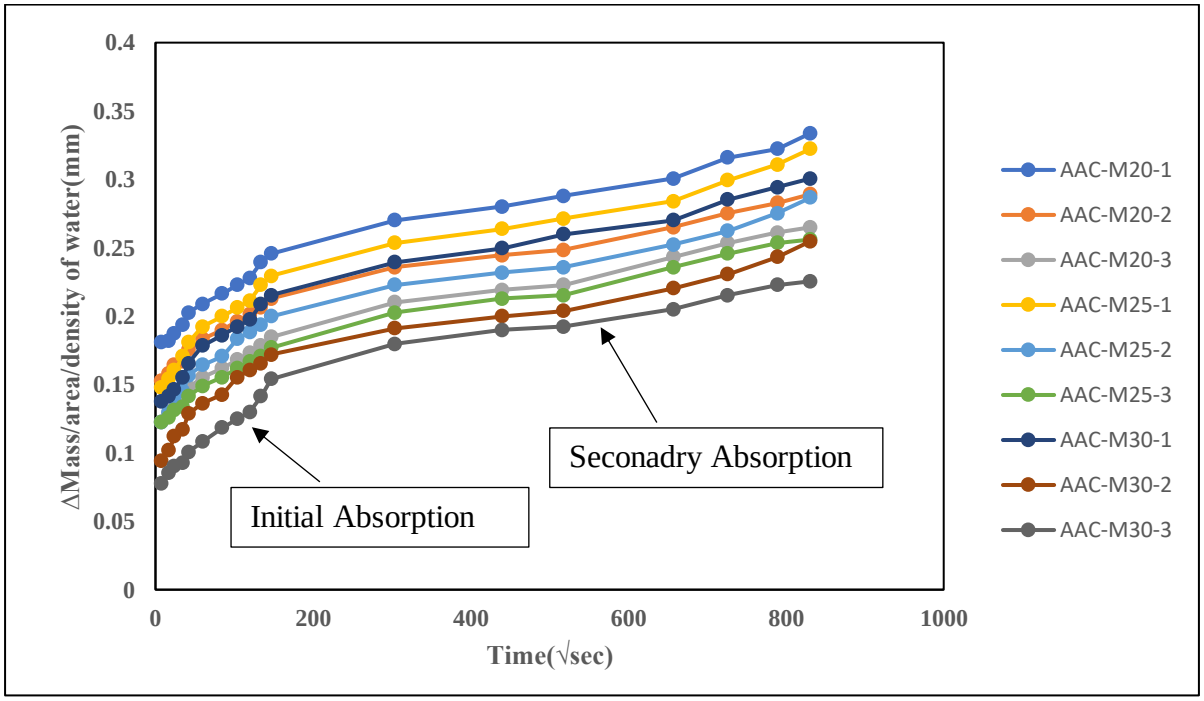

Fig. 4.6- Comparison of Sorptivity Test Results of Sintered Alkali Activated Concrete Specimens

The initial rate of water absorption, measured in mm/$s^{1/2}$, is determined by the slope of the line that best fits the plot of the absorption parameter I against the square root of time ($s^{1/2}$). This slope is calculated using least-squares linear regression analysis of data points collected from 1 minute to 6 hours, excluding any points where the plot shows a clear change in slope. If the data within this timeframe do not exhibit a linear relationship, indicated by a correlation coefficient of less than 0.98, and display systematic curvature, the initial rate of absorption cannot be determined. Similarly, the secondary rate of water absorption is defined as the slope of the line that best fits the plot of I against the square root of time ($s^{1/2}$), using data points from 1 day to 7 days. This slope is also determined using least-squares linear regression. If the data between 1 day and 7 days do not follow a linear relationship (with a correlation coefficient of less than 0.98) and exhibit systematic curvature, the secondary rate of water absorption cannot be established[191]. Fig. 4.7 shows initial water absorption(mm) vs time(√sec) for CC specimens.

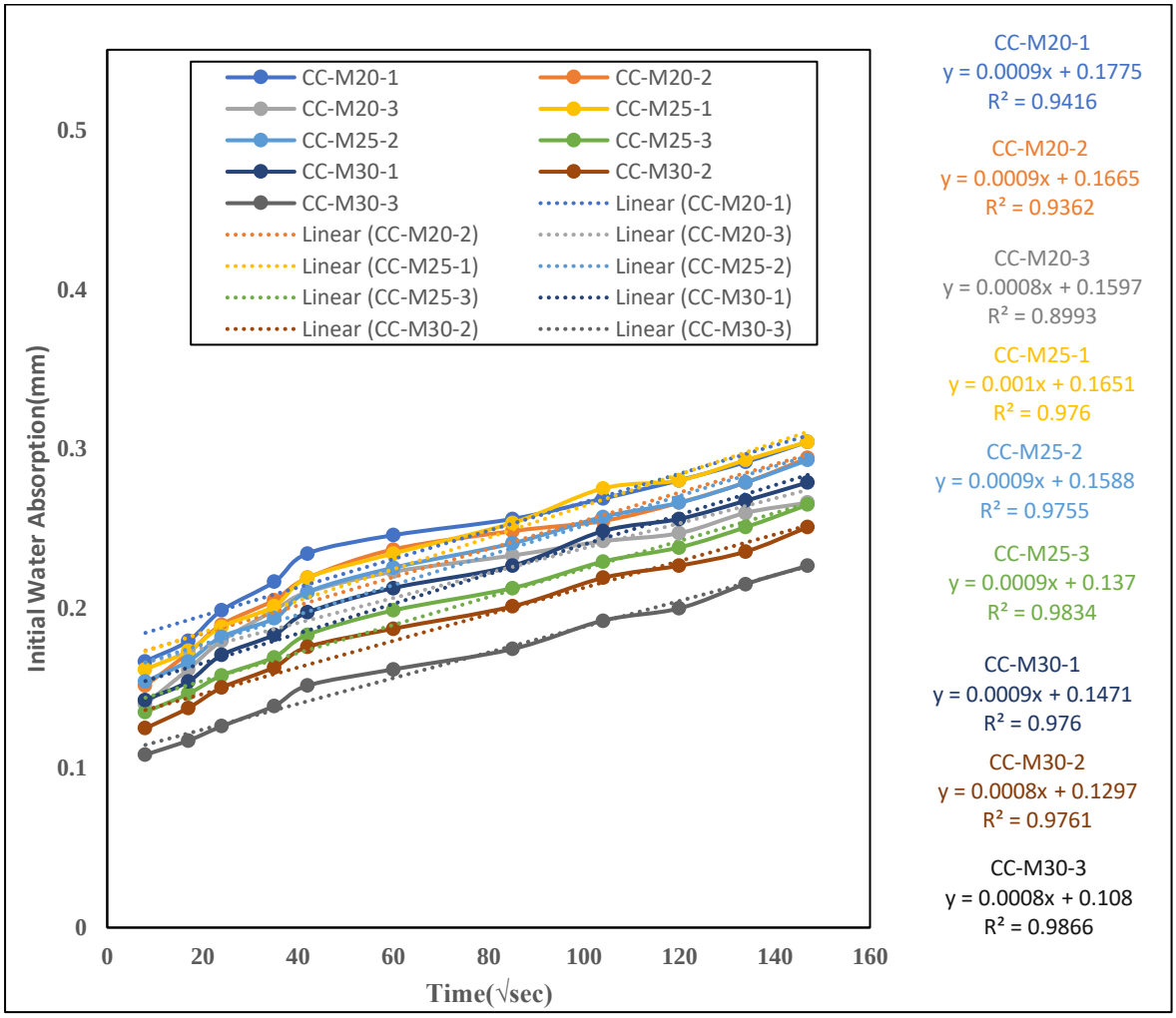

Fig. 4.7- Initial Water Absorption(mm) vs Time(√sec) for Cement Concrete

Initial Water Absorption(mm) (up to 6 hr) vs Time(√sec) for CC and AAC are plotted to get Initial Rate of Absorption. If we draw trendline for all the plots then we will get y= mx +c type straight line where m is rate of initial absorption. The relationship between initial water absorption (mm) and sintering effort is evident from the data, where increasing sintering effort leads to a reduction in initial water absorption. As the sintering process intensifies, either through the application of 20kN pressure or by combining 100°C heating for 5 minutes with 20kN pressure, the slope of the trendlines in the plotted data decreases. This indicates that higher sintering efforts result in lower rates of water absorption, reflecting a more compact and less porous material structure. The consistently high R^2 (coefficient of determination) values across all conditions affirm the strong linear correlation between time and initial water absorption, further emphasizing the effectiveness of sintering in reducing water absorption. Fig. 4.7 shows initial water absorption(mm) vs time(√sec) for AAC specimens.

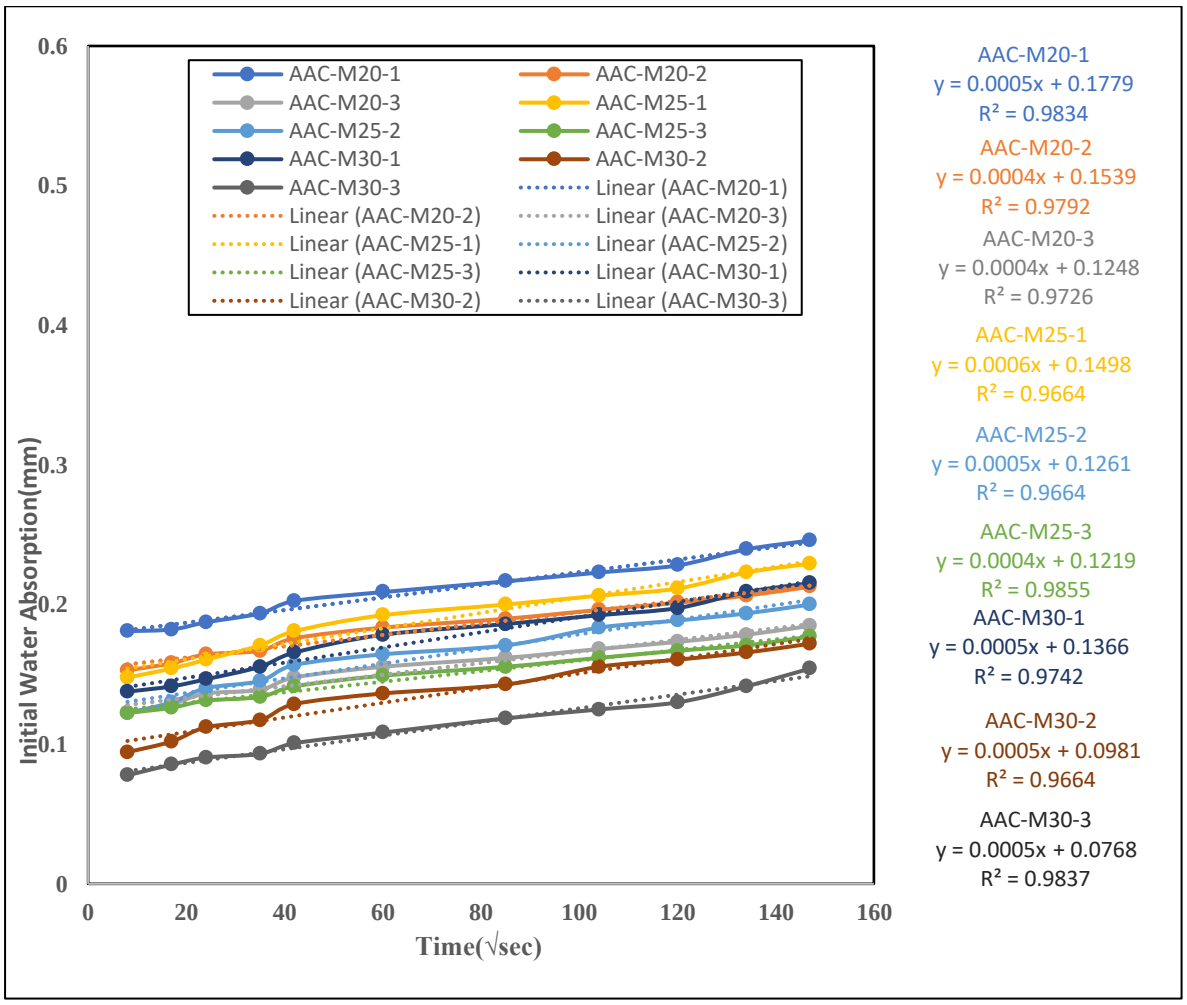

Fig. 4.7- Initial Water Absorption(mm) vs Time(√sec) for Alkali Activated Concrete

4.6 Rapid Chloride Permeability Test (RCPT) Results

The data shows the chloride ion permeability of CC and AAC across grades M20, M25, and M30 under various sintering conditions. For CC, chloride ion permeability remains moderate across all grades and sintering conditions. For the M20 grade, charge passed values decrease from 3664 Coulombs without sintering, to 3219 Coulombs with sintering at 20kN pressure, and further to 2959 Coulombs with full sintering at 100°C for 5 minutes and 20kN pressure. The M25 grade follows a similar trend, with values ranging from 3390 Coulombs without sintering, to 3040 Coulombs with 20kN pressure, and 2948 Coulombs with full sintering. The M30 grade decreases from 3128 Coulombs to 2990 Coulombs, and finally to 2576 Coulombs with full sintering, all rated as moderate permeability.

In AAC, the M20 grade shows a decline in charge passed from 3001 Coulombs without sintering to 2363 Coulombs with 20kN pressure, and 2170 Coulombs with full sintering, maintaining a moderate rating. The M25 grade's charge passed values decrease from 2891 Coulombs to 2250 Coulombs, and further to 1908 Coulombs with full sintering, shifting from moderate to low permeability. For the M30 grade, values drop from 2569 Coulombs to 2120 Coulombs, and to 1683 Coulombs with full sintering, transitioning from moderate to low permeability. This data highlights that enhanced sintering conditions tend to reduce chloride ion permeability, particularly for AAC. Fig. 4.8- comparison of rapid chloride permeability test results sintered CC and AAC specimens.

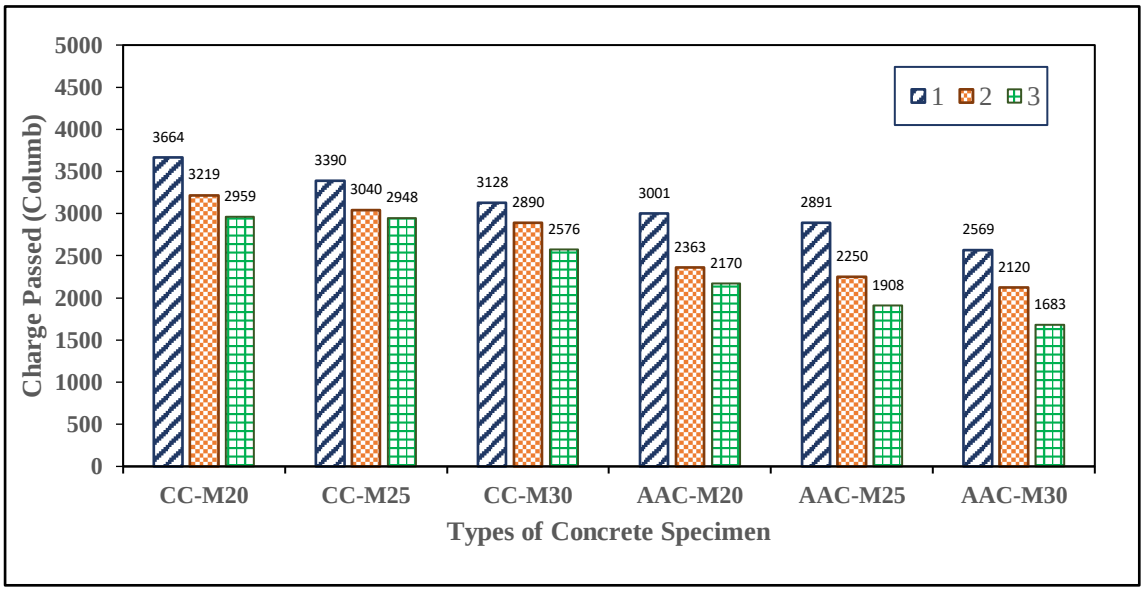

Fig. 4.8- Comparison of Rapid Chloride Permeability Test (RCPT) Results Sintered Cement Concrete and Alkali Activated Concrete Specimens.

4.7 Microstructural Study using Optical Microscope and Image J Software Results

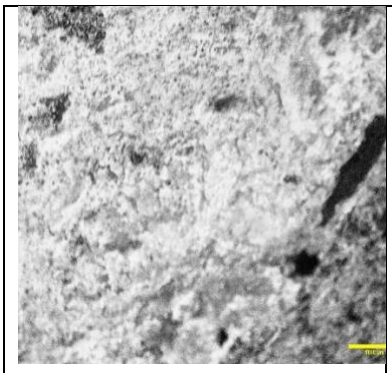	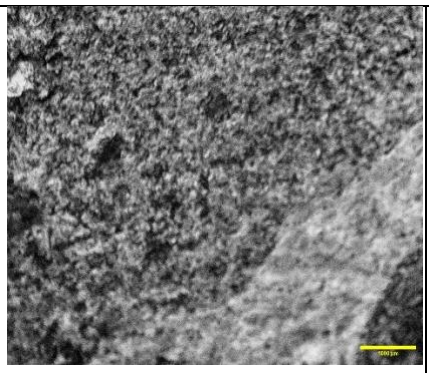	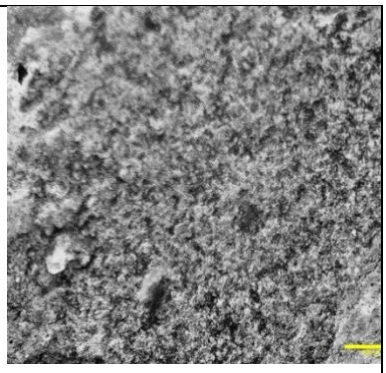
CC-M20-1	CC-M20-2	CC-M20-3
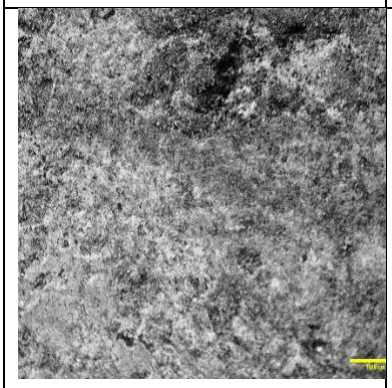	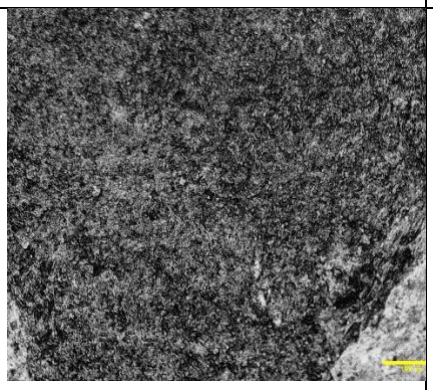	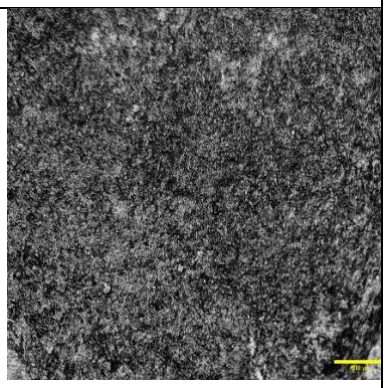
CC-M25-1	CC-M25-2	CC-M25-3
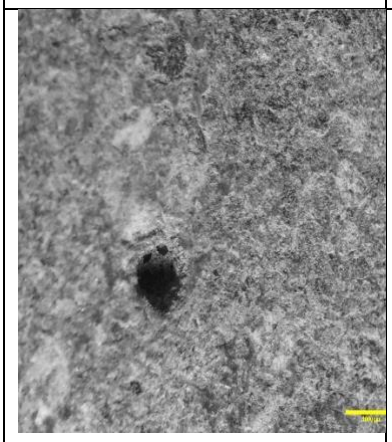	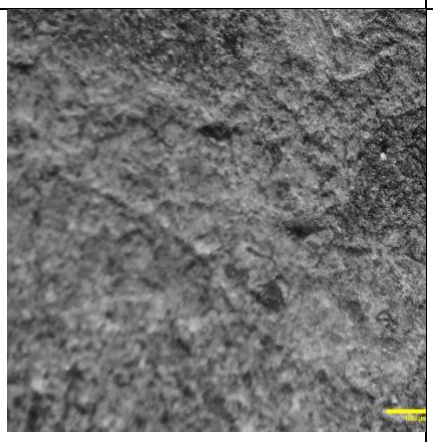	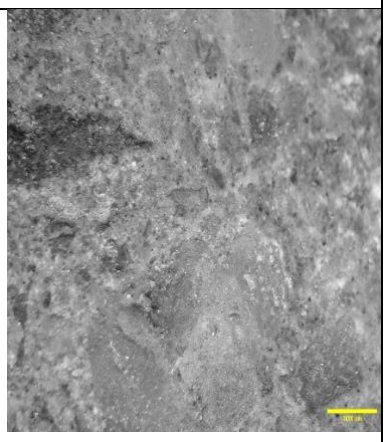
CC-M30-1	CC-M30-2	CC-M30-3

Fig. 4.9- Optical Microscope Images of Different Sintered Cement Concrete Specimens

The ImageJ software analysis of concrete images indicates that as sintering conditions become more rigorous, the porosity of the concrete significantly decreases. Under minimal sintering conditions, the CC and AAC exhibits higher porosity. As the sintering effort is increased to

include moderate pressure, there is a marked reduction in porosity. This trend continues with even more advanced sintering conditions, which involve both elevated temperature and pressure, leading to the lowest porosity values. This pattern demonstrates that enhanced sintering techniques effectively improve the density and reduce the porosity of the CC and AAC.The lowest porosity achieved under elevated temperature and pressure for AAC. Optical microscope images of different sintered CC and AAC specimens fig. 4.9 and 4.10 respectively. Fig. 4.11 shows comparison of porosity(%) of sintered CC and AAC specimens .

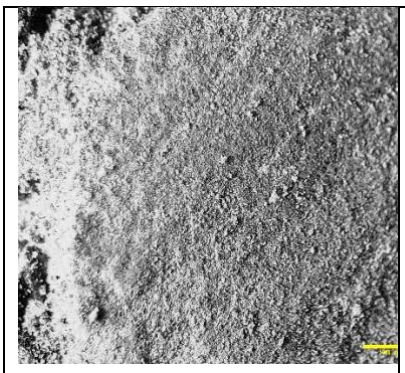	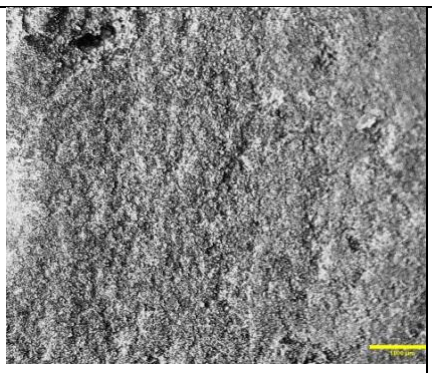	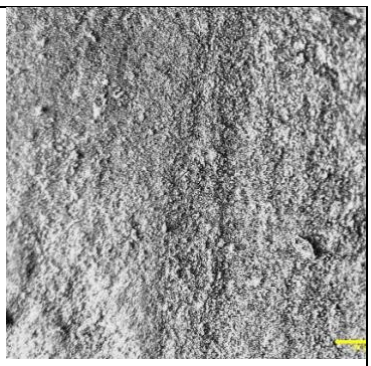
AAC-M20-1	AAC-M20-2	AAC-M20-3
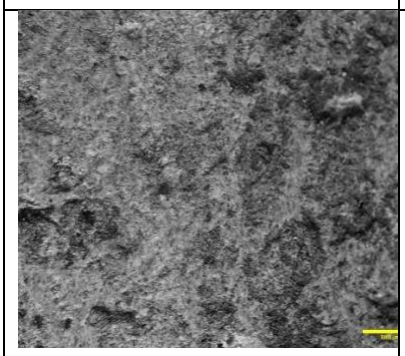	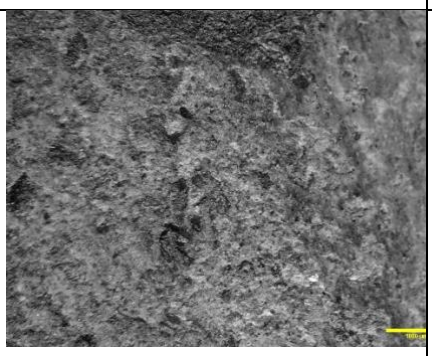	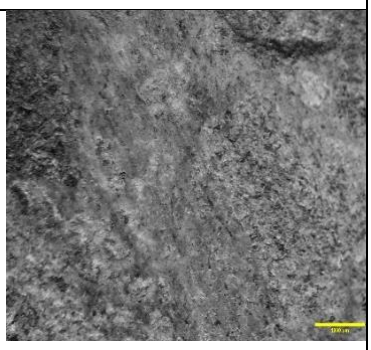
AAC-M25-1	AAC-M25-2	AAC-M25-3
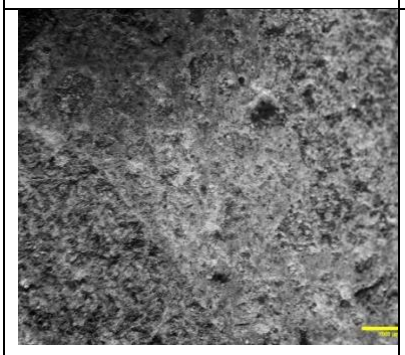		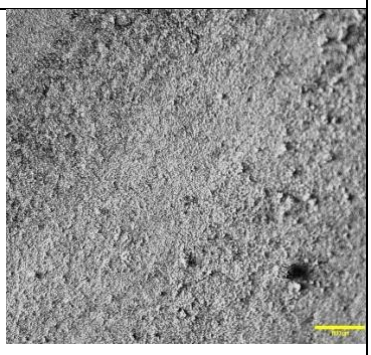
AAC-M30-1	AAC-M30-2	AAC-M30-3

Fig. 4.10- Optical Microscope Images of Different Sintered Alkali Activated Concrete Specimens

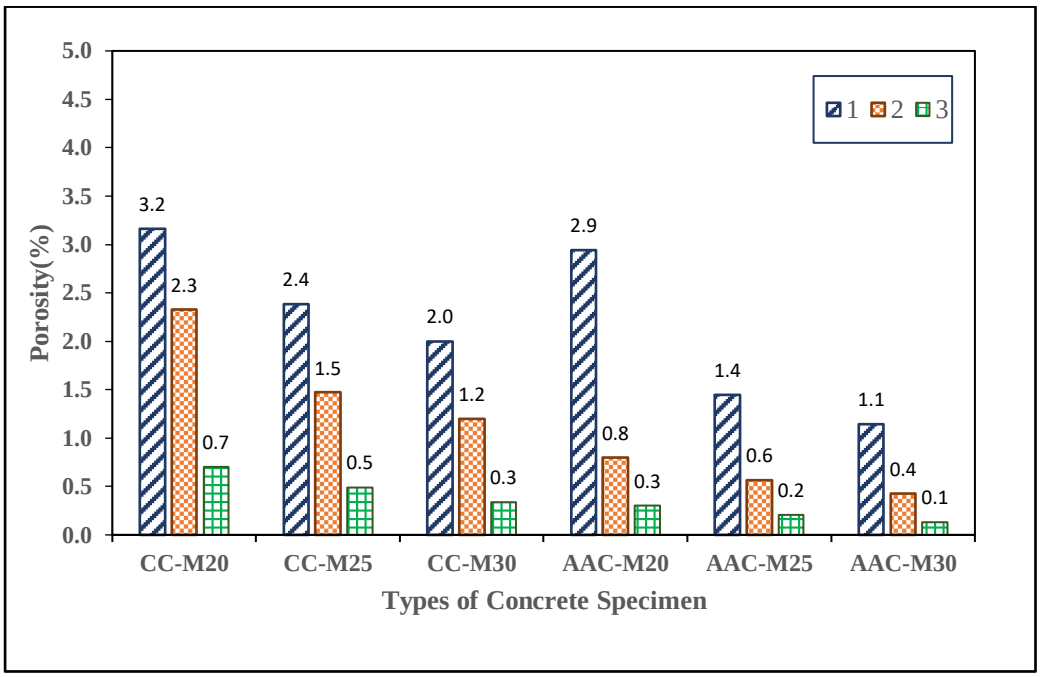

Fig. 4.11- Comparison of Porosity(%) of Sintered Cement Concrete and Alkali Activated Concrete Specimens

4.8 Relationship between Compressive Strength & Porosity

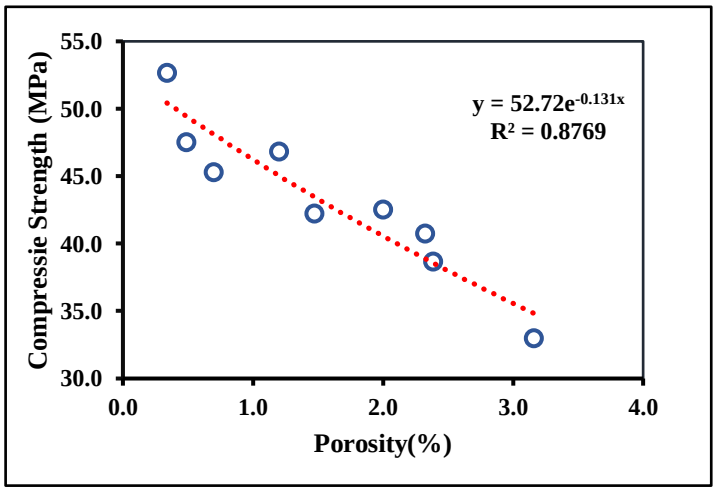

Fig. 4.12- Relationship between Compressive Strength & Porosity of Sintered Cement Concrete

To get the relationship between compressive strength and porosity we need to plot compressive strength vs porosity as scatter plot and draw the trendline. For CC the relationship between compressive strength (in MPa) and porosity (in %) is represented in fig. 4.12 by an exponential decay equation: $y=52.72e^{-0.131x}$ where y represents the compressive strength (MPa), x represents the porosity (%). The equation indicates that as porosity increases, the compressive strength decreases exponentially. The coefficient of determination ($R^2=0.8769$) suggests that about 87.69% of the variance in compressive strength can be explained by the model, indicating a strong negative correlation between porosity and compressive strength.

Fig. 4.13 shows a graph depicting the relationship between compressive strength (in MPa) and porosity. The relationship is expressed by a power-law equation: $y=39.965x^{-0.138}$ where y represents the compressive strength (MPa), x represents the porosity. This equation suggests that as porosity increases, compressive strength decreases according to a power-law relationship. The coefficient of determination ($R^2=0.8765$) indicates that approximately 87.65% of the variance in compressive strength can be explained by the model, signifying a strong inverse correlation between porosity and compressive strength.

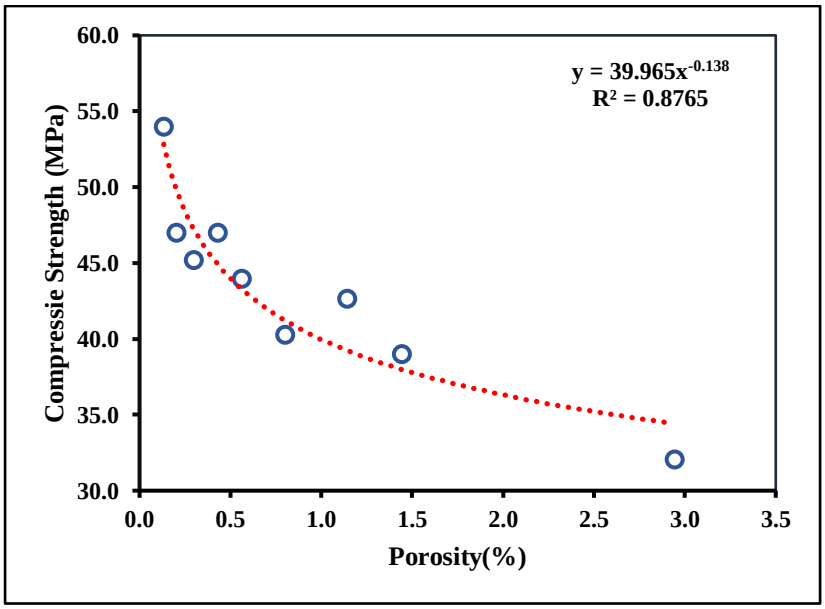

Fig. 4.13 - Relationship between Compressive Strength & Porosity of Sintered Alkali Activated Concrete

Chapter 5

5. Conclusion

5.1 General

The research concludes that sintering holds substantial promise for advancing concrete technology, particularly through its impact on both CC and AAC. The study highlights that sintering significantly enhances the mechanical strength, durability, and overall performance of concrete by optimizing compressive and split tensile strengths. Sintering processes offer innovative ways to improve material efficiency and sustainability, aligning with environmental goals by reducing reliance on traditional Portland cement and utilizing industrial by-products [195]–[197]. The findings emphasize that sintering not only advances the theoretical understanding of concrete properties but also has practical implications for developing more resilient and sustainable construction materials. However, the research also points to the need for further investigation into long-term durability, environmental impacts, and the scalability of sintering methods. Addressing these areas will be crucial for the broader adoption of sintered concrete in real-world applications, ultimately contributing to a more sustainable and resilient construction industry.

5.2 Major Findings

The major findings of this research reveal the substantial impact of sintering on the properties of both CC and AAC. The study demonstrates that sintering, especially under elevated temperatures and pressures, significantly improves the compressive strength, split tensile strength, and overall durability of these concrete types. Notably, AAC exhibits superior mechanical properties and environmental resistance compared to CC, yet sintering enhances both in a promising way. The research identifies specific sintering parameters—such as temperature and duration—as crucial for optimizing concrete performance. It also highlights the advantages of using various material combinations during sintering, which can lead to customized concrete formulations with enhanced characteristics. Advanced characterization techniques have provided deeper insights into microstructural changes and phase formations during sintering. Furthermore, the study underscores the potential of sintering to advance sustainability in construction by improving material efficiency and reducing waste. Overall, these findings suggest that sintering could play a key role in enhancing concrete technology and supporting environmental goals, though further research is needed to address long-term

effects, practical applications, and the development of cost-effective and eco-friendly sintering processes.

5.3 Limitations

Despite the promising results of this research, several limitations must be acknowledged. Firstly, the scope of the study was restricted to specific grades of concrete (M20, M25, M30), which may not fully represent the performance of sintering techniques across a broader range of concrete formulations. Additionally, the research focused primarily on mechanical properties and basic durability tests, potentially overlooking other critical factors such as long-term environmental impacts and economic feasibility of implementing sintering in large-scale production. The study also utilized a limited set of sintering conditions (20kN pressure and 100°C for 5 minutes), which may not encompass all possible variations that could affect concrete performance. Furthermore, while the research highlights improved properties in both CC and AAC, it does not explore the potential challenges and costs associated with integrating sintering techniques into existing construction practices. These drawbacks suggest the need for further investigation into a wider range of concrete grades, sintering conditions, and practical implications to fully assess the viability and benefits of sintering in concrete technology.

5.4 Future Scope

The future of sintering in concrete offers significant potential for innovation and optimization. By fine-tuning sintering parameters, exploring new material combinations, and advancing multi-material techniques, we can enhance concrete's mechanical and structural properties. Advanced characterization tools will deepen our understanding of microstructural changes, while studies on long-term sustainability will evaluate environmental impacts. Integrating AI for efficient production, setting industry standards, and refining material designs are essential for practical application. Future research could expand to include more concrete grades and various sintering conditions, optimizing properties and exploring the environmental and economic aspects for large-scale implementation.

References

[1] Hamsashree, P. Pandit, S. Prashanth, and D. N. Katpady, "Durability of alkali-activated fly ash-slag concrete- state of art," *Innov. Infrastruct. Solut.*, vol. 9, no. 6, pp. 1–21, 2024, doi: 10.1007/s41062-024-01530-5.

[2] N. Zainudeen and J. Jeyamathan, "Cement and its effect to the environment: A case study in SriLanka," *Proc. from Int. Conf. Build. Educ. Res.*, vol. 15, pp. 1408–1416, 2008, [Online]. Available: http://www.irbnet.de/daten/iconda/CIB11336.pdf

[3] H. Page, *Design and Control of Concrete Mixtures, EB001*, no. 54048. 1996.

[4] B. B. Mitikie and D. T. Waldtsadik, "Partial Replacement of Cement by Waste Paper Pulp Ash and Its Effect on Concrete Properties," *Adv. Civ. Eng.*, vol. 2022, pp. 1–12, Feb. 2022, doi: 10.1155/2022/8880196.

[5] K. L. Scrivener, V. M. John, and E. M. Gartner, "Eco-efficient cements: Potential economically viable solutions for a low-CO2 cement-based materials industry," *Cem. Concr. Res.*, vol. 114, no. February, pp. 2–26, 2018, doi: 10.1016/j.cemconres.2018.03.015.

[6] J. L. Provis and S. A. Bernal, "Geopolymers and related alkali-activated materials," *Annu. Rev. Mater. Res.*, vol. 44, pp. 299–327, 2014, doi: 10.1146/annurev-matsci-070813-113515.

[7] I. Garcia-Lodeiro, S. Donatello, A. Fernández-Jiménez, and Á. Palomo, "Hydration of hybrid alkaline cement containing a very large proportion of fly ash: A descriptive model," *Materials (Basel).*, vol. 9, no. 8, 2016, doi: 10.3390/MA9070605.

[8] K. Arbi, M. Nedeljković, Y. Zuo, and G. Ye, "A Review on the Durability of Alkali-Activated Fly Ash/Slag Systems: Advances, Issues, and Perspectives," *Ind. Eng. Chem. Res.*, vol. 55, no. 19, pp. 5439–5453, May 2016, doi: 10.1021/acs.iecr.6b00559.

[9] V. Bilek, O. Sucharda, and D. Bujdos, "Frost resistance of alkali-activated concrete—an important pillar of their sustainability," *Sustain.*, vol. 13, no. 2, pp. 1–13, 2021, doi: 10.3390/su13020473.

[10] M. M. A. Elahi, M. M. Hossain, M. R. Karim, M. F. M. Zain, and C. Shearer, "A review on alkali-activated binders: Materials composition and fresh properties of concrete,"

Constr. Build. Mater., vol. 260, p. 119788, 2020, doi: 10.1016/j.conbuildmat.2020.119788.

[11] I. Pol Segura, N. Ranjbar, A. Juul Damø, L. Skaarup Jensen, M. Canut, and P. Arendt Jensen, "A review: Alkali-activated cement and concrete production technologies available in the industry," *Heliyon*, vol. 9, no. 5, 2023, doi: 10.1016/j.heliyon.2023.e15718.

[12] N. Ranjbar, C. Kuenzel, J. Spangenberg, and M. Mehrali, "Hardening evolution of geopolymers from setting to equilibrium: A review," *Cem. Concr. Compos.*, vol. 114, p. 103729, 2020, doi: 10.1016/j.cemconcomp.2020.103729.

[13] M. Torres-Carrasco and F. Puertas, "Waste glass in the geopolymer preparation. Mechanical and microstructural characterisation," *J. Clean. Prod.*, vol. 90, pp. 397–408, 2015, doi: 10.1016/j.jclepro.2014.11.074.

[14] F. Puertas and M. Torres-Carrasco, "Use of glass waste as an activator in the preparation of alkali-activated slag. Mechanical strength and paste characterisation," *Cem. Concr. Res.*, vol. 57, pp. 95–104, 2014, doi: 10.1016/j.cemconres.2013.12.005.

[15] S. Mujeeb, M. Samudrala, B. A. Lanjewar, R. Chippagiri, M. Kamath, and R. V. Ralegaonkar, "Development of Alkali-Activated 3D Printable Concrete: A Review," *Energies*, vol. 16, no. 10, 2023, doi: 10.3390/en16104181.

[16] J. L. Provis, "Alkali-activated materials," *Cem. Concr. Res.*, vol. 114, pp. 40–48, 2018, doi: 10.1016/j.cemconres.2017.02.009.

[17] V. Živica, M. T. Palou, and M. Križma, "Geopolymer Cements and Their Properties: A Review," *Build. Res. J.*, vol. 61, no. 2, pp. 85–100, 2015, doi: 10.2478/brj-2014-0007.

[18] J. Moon *et al.*, "Characterization of natural pozzolan-based geopolymeric binders," *Cem. Concr. Compos.*, vol. 53, pp. 97–104, 2014, doi: 10.1016/j.cemconcomp.2014.06.010.

[19] B. C. McLellan, R. P. Williams, J. Lay, A. Van Riessen, and G. D. Corder, "Costs and carbon emissions for geopolymer pastes in comparison to ordinary portland cement," *J. Clean. Prod.*, vol. 19, no. 9–10, pp. 1080–1090, 2011, doi: 10.1016/j.jclepro.2011.02.010.

[20] T. Luukkonen, Z. Abdollahnejad, J. Yliniemi, P. Kinnunen, and M. Illikainen, "One-

part alkali-activated materials: A review," *Cem. Concr. Res.*, vol. 103, no. October 2017, pp. 21–34, 2018, doi: 10.1016/j.cemconres.2017.10.001.

[21] F. T. Mahi and O.-H. Kwon, "Liquid Phase Sintering: Ceramics," *Ref. Modul. Mater. Sci. Mater. Eng.*, no. July 2015, pp. 1–6, 2016, doi: 10.1016/b978-0-12-803581-8.03586-4.

[22] K. Dong and X. Wang, "Co2 utilization in the ironmaking and steelmaking process," *Metals (Basel).*, vol. 9, no. 3, pp. 1–8, 2019, doi: 10.3390/met9030273.

[23] L. Cui *et al.*, "Environmental and economic impact assessment of three sintering flue gas treatment technologies in the iron and steel industry," *J. Clean. Prod.*, vol. 311, no. x, p. 127703, 2021, doi: 10.1016/j.jclepro.2021.127703.

[24] M. Rahimian, N. Ehsani, N. Parvin, and H. reza Baharvandi, "The effect of particle size, sintering temperature and sintering time on the properties of Al-Al2O3 composites, made by powder metallurgy," *J. Mater. Process. Technol.*, vol. 209, no. 14, pp. 5387–5393, 2009, doi: 10.1016/j.jmatprotec.2009.04.007.

[25] G. Herranz, A. Romero, V. De Castro, and G. P. Rodríguez, "Development of high speed steel sintered using concentrated solar energy," *J. Mater. Process. Technol.*, vol. 213, no. 12, pp. 2065–2073, 2013, doi: 10.1016/j.jmatprotec.2013.06.002.

[26] J. H. Tsai, K. H. Lin, C. Y. Chen, J. Y. Ding, C. G. Choa, and H. L. Chiang, "Chemical constituents in particulate emissions from an integrated iron and steel facility," *J. Hazard. Mater.*, vol. 147, no. 1–2, pp. 111–119, 2007, doi: 10.1016/j.jhazmat.2006.12.054.

[27] A. N. Chatterjee, S. Kumar, P. Saha, P. K. Mishra, and A. Roy Choudhury, "An experimental design approach to selective laser sintering of low carbon steel," *J. Mater. Process. Technol.*, vol. 136, no. 1–3, pp. 151–157, 2003, doi: 10.1016/S0924-0136(03)00132-8.

[28] K. He and L. Wang, "A review of energy use and energy-efficient technologies for the iron and steel industry," *Renew. Sustain. Energy Rev.*, vol. 70, no. September 2016, pp. 1022–1039, 2017, doi: 10.1016/j.rser.2016.12.007.

[29] S. K. Gupta, A. Prasad, A. Chatterjee, M. Kumar, S. Ghosh, and R. Datta, "Adoption of Sinter Addition in Steelmaking Converter to Control Spitting," *J. Metall.*, vol. 2015, pp.

1–5, 2015, doi: 10.1155/2015/187042.

[30] V. F. De Oliveira and M. C. Bagatini, “Experimental evaluation of the usage of residues for sintermaking,” *J. Mater. Res. Technol.*, vol. 8, no. 6, pp. 5781–5789, 2019, doi: 10.1016/j.jmrt.2019.09.047.

[31] G. Goller, F. N. Oktar, H. Demirkiran, and E. Demirkesen, “Sintering effects on mechanical properties of bioglass reinforced hydroxyapatite composites,” *Key Eng. Mater.*, vol. 240–242, pp. 939–942, 2003, doi: 10.4028/www.scientific.net/kem.240-242.939.

[32] L. Jiang, Y. Liao, Q. Wan, and W. Li, “Effects of sintering temperature and particle size on the translucency of zirconium dioxide dental ceramic,” *J. Mater. Sci. Mater. Med.*, vol. 22, no. 11, pp. 2429–2435, 2011, doi: 10.1007/s10856-011-4438-9.

[33] L. Qiao, H. Zhou, H. Xue, and S. Wang, “Effect of Y2O3 on low temperature sintering and thermal conductivity of AIN ceramics,” *J. Eur. Ceram. Soc.*, vol. 23, no. 1, pp. 61–67, 2003, doi: 10.1016/S0955-2219(02)00079-1.

[34] A. Polotai, K. Breece, E. Dickey, C. Randall, and A. Ragulya, “A novel approach to sintering nanocrystalline barium titanate ceramics,” *J. Am. Ceram. Soc.*, vol. 88, no. 11, pp. 3008–3012, 2005, doi: 10.1111/j.1551-2916.2005.00552.x.

[35] E. A. Olevsky, V. Tikare, and T. Garino, “Multi-scale study of sintering: A review,” *J. Am. Ceram. Soc.*, vol. 89, no. 6, pp. 1914–1922, 2006, doi: 10.1111/j.1551-2916.2006.01054.x.

[36] A. Chatterjee, T. Basak, and K. G. Ayappa, “Analysis of microwave sintering of ceramics,” *AIChE J.*, vol. 44, no. 10, pp. 2302–2311, 1998, doi: 10.1002/aic.690441019.

[37] S. Venzke, R. B. Van Dover, J. M. Phillips, E. M. Gyorgy, T. Siegrist, and C. Chen, “Materials research,” vol. 11, no. 5, pp. 1187–1198, 1996.

[38] M. J. Kim, J. S. Ahn, J. H. Kim, H. Y. Kim, and W. C. Kim, “Effects of the sintering conditions of dental zirconia ceramics on the grain size and translucency,” *J. Adv. Prosthodont.*, vol. 5, no. 2, pp. 161–166, 2013, doi: 10.4047/jap.2013.5.2.161.

[39] K. Maca, V. Pouchly, and P. Zalud, “Two-Step Sintering of oxide ceramics with various crystal structures,” *J. Eur. Ceram. Soc.*, vol. 30, no. 2, pp. 583–589, 2010, doi: 10.1016/j.jeurceramsoc.2009.06.008.

[40] D. Sohrabi Baba Heidary, M. Lanagan, and C. A. Randall, “Contrasting energy efficiency in various ceramic sintering processes,” *J. Eur. Ceram. Soc.*, vol. 38, no. 4, pp. 1018–1029, 2018, doi: 10.1016/j.jeurceramsoc.2017.10.015.

[41] R. E. Dillon, L. A. Matheson, and E. B. Bradford, “Sintering of synthetic latex particles,” *J. Colloid Sci.*, vol. 6, no. 2, pp. 108–117, 1951, doi: 10.1016/0095-8522(51)90031-1.

[42] G. V. Salmoria, J. L. Leite, R. A. Paggi, A. Lago, and A. T. N. Pires, “Selective laser sintering of PA12/HDPE blends: Effect of components on elastic/plastic behavior,” *Polym. Test.*, vol. 27, no. 6, pp. 654–659, 2008, doi: 10.1016/j.polymertesting.2008.04.007.

[43] R. D. Goodridge, R. J. M. Hague, and C. J. Tuck, “An empirical study into laser sintering of ultra-high molecular weight polyethylene (UHMWPE),” *J. Mater. Process. Technol.*, vol. 210, no. 1, pp. 72–80, 2010, doi: 10.1016/j.jmatprotec.2009.08.016.

[44] T. L. Starr, T. J. Gornet, and J. S. Usher, “The effect of process conditions on mechanical properties of laser-sintered nylon,” *Rapid Prototyp. J.*, vol. 17, no. 6, pp. 418–423, 2011, doi: 10.1108/13552541111184143.

[45] Y. Shi, Z. Li, H. Sun, S. Huang, and F. Zeng, “Effect of the properties of the polymer materials on the quality of selective laser sintering parts,” *Proc. Inst. Mech. Eng. Part L J. Mater. Des. Appl.*, vol. 218, no. 3, pp. 247–252, 2004, doi: 10.1243/1464420041579454.

[46] S. K. Tiwari, S. Pande, S. Agrawal, and S. M. Bobade, “Selection of selective laser sintering materials for different applications,” *Rapid Prototyp. J.*, vol. 21, no. 6, pp. 630–648, 2015, doi: 10.1108/RPJ-03-2013-0027.

[47] W. Ruban, V. Vijayakumar, P. Dhanabal, and T. Pridhar, “Effective process parameters in selective laser sintering,” *Int. J. Rapid Manuf.*, vol. 4, no. 2/3/4, p. 148, 2014, doi: 10.1504/ijrapidm.2014.066036.

[48] T. Miyasaka, M. Ikegami, and Y. Kijitori, “Photovoltaic Performance of Plastic Dye-Sensitized Electrodes Prepared by Low-Temperature Binder-Free Coating of Mesoscopic Titania,” *J. Electrochem. Soc.*, vol. 154, no. 5, p. A455, 2007, doi: 10.1149/1.2712140.

[49] H. C. H. Ho, I. Gibson, and W. L. Cheung, “Effects of energy density on morphology

and properties of selective laser sintered polycarbonate," *J. Mater. Process. Technol.*, vol. 89–90, pp. 204–210, 1999, doi: 10.1016/S0924-0136(99)00007-2.

[50] J. D. B. De Mello, C. Binder, G. Hammes, R. Binder, and A. N. Klein, "Tribological behaviour of sintered iron based self-lubricating composites," *Friction*, vol. 5, no. 3, pp. 285–307, 2017, doi: 10.1007/s40544-017-0186-2.

[51] J. D. B. De Mello, C. Binder, R. Binder, and A. N. Klein, "Effect of precursor content and sintering temperature on the scuffing resistance of sintered self lubricating steel," *Wear*, vol. 271, no. 9–10, pp. 1862–1867, 2011, doi: 10.1016/j.wear.2010.11.038.

[52] L. Yeong-Jae, L. Kwang-Hee, and L. Chul-Hee, "Self-lubricating and friction performance of a three-dimensional- printed journal bearing," *J. Tribol.*, vol. 140, no. 5, 2018, doi: 10.1115/1.4039995.

[53] P. S. Gajjal and G. S. Lathkar, "Wear behaviour of sintered bearings using additives in dry sliding," *Mater. Today Proc.*, vol. 46, pp. 2483–2488, 2021, doi: 10.1016/j.matpr.2021.01.413.

[54] J. D. B. De Mello, C. Binder, A. N. Klein, and R. Binder, "Effect of sintering temperature on the tribological behavior of plasma assisted debinded and sintered mim self lubricating steels," *ASME 2010 10th Bienn. Conf. Eng. Syst. Des. Anal. ESDA2010*, vol. 1, pp. 373–380, 2010, doi: 10.1115/ESDA2010-24245.

[55] C. Teisanu and S. Gheorghe, "Development of new PM iron-based materials for self-lubricating bearings," *Adv. Tribol.*, vol. 2011, 2011, doi: 10.1155/2011/248037.

[56] R. Gangarde, R. R. Kharde, and A. Jagtap, "REVIEW ON PARAMETER OPTIMIZATION OF SELF".

[57] C. Binder, T. Bendo, R. V. Pereira, G. Hammes, J. D. B. de Mello, and A. N. Klein, "Influence of the SiC content and sintering temperature on the microstructure, mechanical properties and friction behaviour of sintered self-lubricating composites," *Powder Metall.*, vol. 59, no. 5, pp. 384–393, 2016, doi: 10.1080/00325899.2016.1250036.

[58] C. D. Desforges, "Sintered materials for electrical contacts," *Powder Metall.*, vol. 22, no. 3, pp. 138–144, 1979, doi: 10.1179/pom.1979.22.3.138.

[59] S. K. Jha and R. Raj, "The effect of electric field on sintering and electrical conductivity

of Titania," *J. Am. Ceram. Soc.*, vol. 97, no. 2, pp. 527–534, 2014, doi: 10.1111/jace.12682.

[60] F. Thiimmler and W. Thomma, "REVIEW 115 The sintering process," *Metall. Rev.*, pp. 69–108, 1949.

[61] S. Grasso *et al.*, "A review of cold sintering processes," *Adv. Appl. Ceram.*, vol. 119, no. 3, pp. 115–143, 2020, doi: 10.1080/17436753.2019.1706825.

[62] C. Baud, "Sintering Jos e," pp. 865–878.

[63] H. E. Exner and E. Arzt, "Sintering Processes," *Sinter. Key Pap.*, pp. 157–184, 1990, doi: 10.1007/978-94-009-0741-6_10.

[64] S.-J. L. Kang, "Sintering Processes," *Sintering*, pp. 3–8, 2005, doi: 10.1016/b978-075066385-4/50001-7.

[65] H. E. EXNER and E. ARZT, "Sintering Processes," *Phys. Metall.*, pp. 2627–2662, 1996, doi: 10.1016/b978-044489875-3/50036-3.

[66] M. N. Rahaman, "Sintering of ceramics," *Sinter. Ceram.*, pp. 1–389, 2007, doi: 10.1201/b15869-2.

[67] M. Verma, N. Dev, I. Rahman, M. Nigam, M. Ahmed, and J. Mallick, "Geopolymer Concrete: A Material for Sustainable Development in Indian Construction Industries," *Crystals*, vol. 12, no. 4, pp. 1–24, 2022, doi: 10.3390/cryst12040514.

[68] T. Note, "Technical Note PROPERTIES OF ALKALI-ACTIVATED FLY ASH CONCRETE," vol. 10, no. 1, pp. 57–64, 2013.

[69] A. Palomo, M. W. Grutzeck, and M. T. Blanco, "Alkali-activated fly ashes: A cement for the future," *Cem. Concr. Res.*, vol. 29, no. 8, pp. 1323–1329, 1999, doi: 10.1016/S0008-8846(98)00243-9.

[70] A. Fernández-Jiménez and A. Palomo, "Composition and microstructure of alkali activated fly ash binder: Effect of the activator," *Cem. Concr. Res.*, vol. 35, no. 10, pp. 1984–1992, 2005, doi: 10.1016/j.cemconres.2005.03.003.

[71] Y. Ding, J. G. Dai, and C. J. Shi, "Mechanical properties of alkali-activated concrete: A state-of-the-art review," *Constr. Build. Mater.*, vol. 127, pp. 68–79, 2016, doi: 10.1016/j.conbuildmat.2016.09.121.

[72] K. Ruengsillapanun, T. Udtaranakron, T. Pulngern, W. Tangchirapat, and C. Jaturapitakkul, “Mechanical properties, shrinkage, and heat evolution of alkali activated fly ash concrete,” *Constr. Build. Mater.*, vol. 299, p. 123954, 2021, doi: 10.1016/j.conbuildmat.2021.123954.

[73] A. Mehta, R. Siddique, T. Ozbakkaloglu, F. Uddin Ahmed Shaikh, and R. Belarbi, “Fly ash and ground granulated blast furnace slag-based alkali-activated concrete: Mechanical, transport and microstructural properties,” *Constr. Build. Mater.*, vol. 257, p. 119548, 2020, doi: 10.1016/j.conbuildmat.2020.119548.

[74] G. Fang, W. K. Ho, W. Tu, and M. Zhang, “Workability and mechanical properties of alkali-activated fly ash-slag concrete cured at ambient temperature,” *Constr. Build. Mater.*, vol. 172, pp. 476–487, 2018, doi: 10.1016/j.conbuildmat.2018.04.008.

[75] F. N. Okoye, J. Durgaprasad, and N. B. Singh, “Mechanical properties of alkali activated flyash/Kaolin based geopolymer concrete,” *Constr. Build. Mater.*, vol. 98, pp. 685–691, 2015, doi: 10.1016/j.conbuildmat.2015.08.009.

[76] B. wan Jo, S. kook Park, and J. bin Park, “Properties of concrete made with alkali-activated fly ash lightweight aggregate (AFLA),” *Cem. Concr. Compos.*, vol. 29, no. 2, pp. 128–135, 2007, doi: 10.1016/j.cemconcomp.2006.09.004.

[77] N. K. Lee and H. K. Lee, “Setting and mechanical properties of alkali-activated fly ash/slag concrete manufactured at room temperature,” *Constr. Build. Mater.*, vol. 47, pp. 1201–1209, Oct. 2013, doi: 10.1016/j.conbuildmat.2013.05.107.

[78] F. Şahin, M. Uysal, and O. Canpolat, “Systematic evaluation of the aggregate types and properties on metakaolin based geopolymer composites,” *Constr. Build. Mater.*, vol. 278, 2021, doi: 10.1016/j.conbuildmat.2021.122414.

[79] G. Görhan, R. Aslaner, and O. Şinik, “The effect of curing on the properties of metakaolin and fly ash-based geopolymer paste,” *Compos. Part B Eng.*, vol. 97, pp. 329–335, 2016, doi: 10.1016/j.compositesb.2016.05.019.

[80] H. Alanazi, M. Yang, D. Zhang, and Z. Gao, “Early strength and durability of metakaolin-based geopolymer concrete,” *Mag. Concr. Res.*, vol. 69, no. 1, pp. 46–54, 2017, doi: 10.1680/jmacr.16.00118.

[81] A. B. Moradikhou, A. Esparham, and M. Jamshidi Avanaki, “Physical & mechanical

properties of fiber reinforced metakaolin-based geopolymer concrete," *Constr. Build. Mater.*, vol. 251, p. 118965, 2020, doi: 10.1016/j.conbuildmat.2020.118965.

[82] A. Albidah, A. S. Alqarni, H. Abbas, T. Almusallam, and Y. Al-Salloum, "Behavior of Metakaolin-Based geopolymer concrete at ambient and elevated temperatures," *Constr. Build. Mater.*, vol. 317, no. August 2021, p. 125910, 2022, doi: 10.1016/j.conbuildmat.2021.125910.

[83] F. A. Shilar, S. V. Ganachari, V. B. Patil, and K. S. Nisar, "Evaluation of structural performances of metakaolin based geopolymer concrete," *J. Mater. Res. Technol.*, vol. 20, pp. 3208–3228, 2022, doi: 10.1016/j.jmrt.2022.08.020.

[84] F. A. Shilar, S. V. Ganachari, V. B. Patil, I. Neelakanta Reddy, and J. Shim, "Preparation and validation of sustainable metakaolin based geopolymer concrete for structural application," *Constr. Build. Mater.*, vol. 371, no. January, p. 130688, 2023, doi: 10.1016/j.conbuildmat.2023.130688.

[85] A. Albidah, M. Alghannam, H. Abbas, T. Almusallam, and Y. Al-Salloum, "Characteristics of metakaolin-based geopolymer concrete for different mix design parameters," *J. Mater. Res. Technol.*, vol. 10, pp. 84–98, 2021, doi: 10.1016/j.jmrt.2020.11.104.

[86] T. Luukkonen, M. Sarkkinen, K. Kemppainen, J. Rämö, and U. Lassi, "Metakaolin geopolymer characterization and application for ammonium removal from model solutions and landfill leachate," *Appl. Clay Sci.*, vol. 119, pp. 266–276, 2016, doi: 10.1016/j.clay.2015.10.027.

[87] R. Pouhet and M. Cyr, "Formulation and performance of flash metakaolin geopolymer concretes," *Constr. Build. Mater.*, vol. 120, pp. 150–160, 2016, doi: 10.1016/j.conbuildmat.2016.05.061.

[88] G. Mounika, B. Ramesh, and J. S. Kalyana Rama, "Experimental investigation on physical and mechanical properties of alkali activated concrete using industrial and agro waste," *Mater. Today Proc.*, vol. 33, pp. 4372–4376, 2020, doi: 10.1016/j.matpr.2020.07.634.

[89] V. S. Athira, V. Charitha, G. Athira, and A. Bahurudeen, "Agro-waste ash based alkali-activated binder: Cleaner production of zero cement concrete for construction," *J. Clean.*

Prod., vol. 286, p. 125429, 2021, doi: 10.1016/j.jclepro.2020.125429.

[90] A. Qudoos, H. G. Kim, Atta-ur-Rehman, and J. S. Ryou, "Effect of mechanical processing on the pozzolanic efficiency and the microstructure development of wheat straw ash blended cement composites," *Constr. Build. Mater.*, vol. 193, pp. 481–490, 2018, doi: 10.1016/j.conbuildmat.2018.10.229.

[91] J. Rivera, F. Castro, A. Fernández-Jiménez, and N. Cristelo, "Alkali-Activated Cements from Urban, Mining and Agro-Industrial Waste: State-of-the-art and Opportunities," *Waste and Biomass Valorization*, vol. 12, no. 5, pp. 2665–2683, 2021, doi: 10.1007/s12649-020-01071-9.

[92] S. Singh, M. M. Dalbehera, S. Maiti, R. S. Bisht, N. B. Balam, and S. K. Panigrahi, "Investigation of agro-forestry and construction demolition wastes in alkali-activated fly ash bricks as sustainable building materials," *Waste Manag.*, vol. 159, no. January, pp. 114–124, 2023, doi: 10.1016/j.wasman.2023.01.031.

[93] Ü. Yurt and F. Bekar, "Comparative study of hazelnut-shell biomass ash and metakaolin to improve the performance of alkali-activated concrete: A sustainable greener alternative," *Constr. Build. Mater.*, vol. 320, no. June 2021, p. 126230, 2022, doi: 10.1016/j.conbuildmat.2021.126230.

[94] S. Shameem Banu, J. Karthikeyan, and P. Jayabalan, "Effect of agro-waste on strength and durability properties of concrete," *Constr. Build. Mater.*, vol. 258, p. 120322, 2020, doi: 10.1016/j.conbuildmat.2020.120322.

[95] E. R. Teixeira, A. Camões, and F. G. Branco, "Synergetic effect of biomass fly ash on improvement of high-volume coal fly ash concrete properties," *Constr. Build. Mater.*, vol. 314, no. May 2021, 2022, doi: 10.1016/j.conbuildmat.2021.125680.

[96] A. Pereira *et al.*, "Mechanical and durability properties of alkali-activated mortar based on sugarcane bagasse ash and blast furnace slag," *Ceram. Int.*, vol. 41, no. 10, pp. 13012–13024, 2015, doi: 10.1016/j.ceramint.2015.07.001.

[97] R. Carrillo-Beltran, F. A. Corpas-Iglesias, J. M. Terrones-Saeta, and M. Bertoya-Sol, "New geopolymers from industrial by-products: Olive biomass fly ash and chamotte as raw materials," *Constr. Build. Mater.*, vol. 272, p. 121924, 2021, doi: 10.1016/j.conbuildmat.2020.121924.

[98] R. Abbas, M. A. Khereby, H. Y. Ghorab, and N. Elkhoshkhany, “Preparation of geopolymer concrete using Egyptian kaolin clay and the study of its environmental effects and economic cost,” *Clean Technol. Environ. Policy*, vol. 22, no. 3, pp. 669–687, 2020, doi: 10.1007/s10098-020-01811-4.

[99] A. S. Bature, M. Khorami, E. Ganjian, and M. Tyrer, “Influence of alkali activator type and proportion on strength performance of calcined clay geopolymer mortar,” *Constr. Build. Mater.*, vol. 267, p. 120446, 2021, doi: 10.1016/j.conbuildmat.2020.120446.

[100] A. M. Okashah, F. F. Zainal, N. F. Hayazi, M. N. Nordin, and A. Abdullah, “Pozzolanic properties of calcined clay in geopolymer concrete: A review,” *AIP Conf. Proc.*, vol. 2339, no. May, 2021, doi: 10.1063/5.0044583.

[101] B. Rath, R. Debnath, A. Paul, P. Velusamy, and D. Balamoorthy, “Performance of natural rubber latex on calcined clay-based glass fiber-reinforced geopolymer concrete,” *Asian J. Civ. Eng.*, vol. 21, no. 6, pp. 1051–1066, 2020, doi: 10.1007/s42107-020-00261-z.

[102] B. Kanagaraj, N. Anand, R. Samuvel Raj, and E. Lubloy, “Techno-socio-economic aspects of Portland cement, Geopolymer, and Limestone Calcined Clay Cement (LC3) composite systems: A-State-of-Art-Review,” *Constr. Build. Mater.*, vol. 398, no. June, 2023, doi: 10.1016/j.conbuildmat.2023.132484.

[103] K. Boakye and M. Khorami, “Impact of Low-Reactivity Calcined Clay on the Performance of Fly Ash-Based Geopolymer Mortar,” *Sustain.*, vol. 15, no. 18, 2023, doi: 10.3390/su151813556.

[104] A. Elimbi, H. K. Tchakoute, and D. Njopwouo, “Effects of calcination temperature of kaolinite clays on the properties of geopolymer cements,” *Constr. Build. Mater.*, vol. 25, no. 6, pp. 2805–2812, 2011, doi: 10.1016/j.conbuildmat.2010.12.055.

[105] A. Gupta, N. Gupta, and K. K. Saxena, “Experimental study of the mechanical and durability properties of Slag and Calcined Clay based geopolymer composite,” *Adv. Mater. Process. Technol.*, vol. 8, no. sup2, pp. 655–669, 2022, doi: 10.1080/2374068X.2021.1948709.

[106] K. Scrivener and A. Favier, “Calcined Clays for Sustainable Concrete,” *RILEM Bookseries*, pp. 359–360, 2015, doi: 10.1007/978-94-017-9939-3.

[107] J. Guru Jawahar, D. Lavanya, and C. Sashidhar, “Performance of fly ash and ggbs based geopolymer concrete in acid environment,” *Int. J. Res. Sci. Innov.*, vol. 3, no. 8, pp. 101–104, 2016.

[108] G. Thakur *et al.*, “Development of GGBS-Based Geopolymer Concrete Incorporated with Polypropylene Fibers as Sustainable Materials,” *Sustain.*, vol. 14, no. 17, pp. 1–24, 2022, doi: 10.3390/su141710639.

[109] F. A. Shilar, S. V. Ganachari, V. B. Patil, S. Javed, T. M. Y. Khan, and R. U. Baig, “Assessment of Destructive and Nondestructive Analysis for GGBS Based Geopolymer Concrete and Its Statistical Analysis,” *Polymers (Basel).*, vol. 14, no. 15, 2022, doi: 10.3390/polym14153132.

[110] B. J. Mathew, M. Sudhakar, and C. Natarajan, “Strength , Economic and Sustainability Characteristics of Coal Ash – GGBS Based Geopolymer Concrete,” *Int. J. Comput. Eng. Res.*, vol. 3, pp. 207–212, 2013.

[111] W. H. Lee, J. H. Wang, Y. C. Ding, and T. W. Cheng, “A study on the characteristics and microstructures of GGBS/FA based geopolymer paste and concrete,” *Constr. Build. Mater.*, vol. 211, pp. 807–813, 2019, doi: 10.1016/j.conbuildmat.2019.03.291.

[112] G. Mallikarjuna Rao and T. D. Gunneswara Rao, “A quantitative method of approach in designing the mix proportions of fly ash and GGBS-based geopolymer concrete,” *Aust. J. Civ. Eng.*, vol. 16, no. 1, pp. 53–63, 2018, doi: 10.1080/14488353.2018.1450716.

[113] K. Chandra Padmakar and B. Sarath Chandra Kumar, “An experimental study on metakaolin and GGBS based geopolymer concrete,” *Int. J. Civ. Eng. Technol.*, vol. 8, no. 1, pp. 544–557, 2017, doi: 10.21817/ijet/2017/v9i1/170902311.

[114] A. A. Shahmansouri, H. Akbarzadeh Bengar, and S. Ghanbari, “Compressive strength prediction of eco-efficient GGBS-based geopolymer concrete using GEP method,” *J. Build. Eng.*, vol. 31, no. February, p. 101326, 2020, doi: 10.1016/j.jobe.2020.101326.

[115] S. V Patil, V. B. Karikatti, and M. Chitawadagi, “Granulated Blast-Furnace Slag (GGBS) based Geopolymer Concrete - Review,” vol. 5, no. 1, 2018.

[116] A. Bouaissi, L. yuan Li, M. M. Al Bakri Abdullah, and Q. B. Bui, “Mechanical properties and microstructure analysis of FA-GGBS-HMNS based geopolymer concrete,” *Constr. Build. Mater.*, vol. 210, pp. 198–209, 2019, doi:

10.1016/j.conbuildmat.2019.03.202.

[117] B. Rajini and C. Sashidhar, “Prediction mechanical properties of GGBS based on geopolymer concrete by using analytical method,” *Mater. Today Proc.*, vol. 19, no. xxxx, pp. 536–540, 2019, doi: 10.1016/j.matpr.2019.07.729.

[118] D. K. J. P. Alwis and N. Sakthieswaran, “Strength and stability characteristics of GGBS and red mud based geopolymer concrete incorporated with hybrid fibres,” *Indian Concr. J.*, vol. 89, no. 11, pp. 66–72, 2015.

[119] A. Kumar, T. J. Saravanan, K. Bisht, and K. I. S. A. Kabeer, “A review on the utilization of red mud for the production of geopolymer and alkali activated concrete,” *Constr. Build. Mater.*, vol. 302, no. April, p. 124170, 2021, doi: 10.1016/j.conbuildmat.2021.124170.

[120] J. He, Y. Jie, J. Zhang, Y. Yu, and G. Zhang, “Synthesis and characterization of red mud and rice husk ash-based geopolymer composites,” *Cem. Concr. Compos.*, vol. 37, no. 1, pp. 108–118, 2013, doi: 10.1016/j.cemconcomp.2012.11.010.

[121] U. Zakira, K. Zheng, N. Xie, and B. Birgisson, “Development of high-strength geopolymers from red mud and blast furnace slag,” *J. Clean. Prod.*, vol. 383, no. December 2021, p. 135439, 2023, doi: 10.1016/j.jclepro.2022.135439.

[122] M. Mudgal, A. Singh, R. K. Chouhan, A. Acharya, and A. K. Srivastava, “Fly ash red mud geopolymer with improved mechanical strength,” *Clean. Eng. Technol.*, vol. 4, p. 100215, Oct. 2021, doi: 10.1016/j.clet.2021.100215.

[123] S. Kulkarni, “Experimental Study on Red Mud, Fly Ash and GGBFS based Geopolymer Concrete A Green Substitute to Conventional Concrete,” *Int. J. Eng. Res. Technol.*, vol. 7, no. 2278–0181, pp. 107–111, 2018, [Online]. Available: www.ijert.org

[124] R. R. Bellum, C. Venkatesh, and S. R. C. Madduru, “Influence of red mud on performance enhancement of fly ash-based geopolymer concrete,” *Innov. Infrastruct. Solut.*, vol. 6, no. 4, pp. 1–9, 2021, doi: 10.1007/s41062-021-00578-x.

[125] Z. Xu, Q. Liu, H. Y. Long, H. Deng, Z. Chen, and D. Hui, “Influence of nano-SiO2 and steel fiber on mechanical and microstructural properties of red mud-based geopolymer concrete,” *Constr. Build. Mater.*, vol. 364, no. December 2022, p. 129990, 2023, doi: 10.1016/j.conbuildmat.2022.129990.

[126] S. Ahmed, T. Meng, and M. Taha, “Utilization of red mud for producing a high strength binder by composition optimization and nano strengthening,” *Nanotechnol. Rev.*, vol. 9, no. 1, pp. 396–409, 2020, doi: 10.1515/ntrev-2020-0029.

[127] X. Liang and Y. Ji, “Mechanical properties and permeability of red mud-blast furnace slag-based geopolymer concrete,” *SN Appl. Sci.*, vol. 3, no. 1, pp. 1–10, 2021, doi: 10.1007/s42452-020-03985-4.

[128] Z. Du, S. Sheng, and J. Guo, “Effect of composite activators on mechanical properties, hydration activity and microstructure of red mud-based geopolymer,” *J. Mater. Res. Technol.*, vol. 24, pp. 8077–8085, 2023, doi: 10.1016/j.jmrt.2023.05.049.

[129] A. A. Khalaf and K. Kopecskó, “Properties of red-mud-based geopolymers in the light of their chemical composition,” *J. Phys. Conf. Ser.*, vol. 2315, no. 1, 2022, doi: 10.1088/1742-6596/2315/1/012024.

[130] H. Zhu, G. Liang, J. Xu, Q. Wu, and M. Zhai, “Influence of rice husk ash on the waterproof properties of ultrafine fly ash based geopolymer,” *Constr. Build. Mater.*, vol. 208, pp. 394–401, 2019, doi: 10.1016/j.conbuildmat.2019.03.035.

[131] Y. Y. Kim, B.-J. Lee, V. Saraswathy, and S.-J. Kwon, “Strength and Durability Performance of Alkali-Activated Rice Husk Ash Geopolymer Mortar,” *Sci. World J.*, vol. 2014, pp. 1–10, 2014, doi: 10.1155/2014/209584.

[132] Saloni *et al.*, “Performance of rice husk Ash-Based sustainable geopolymer concrete with Ultra-Fine slag and Corn cob ash,” *Constr. Build. Mater.*, vol. 279, p. 122526, 2021, doi: 10.1016/j.conbuildmat.2021.122526.

[133] S. S. Hossain, P. K. Roy, and C. J. Bae, “Utilization of waste rice husk ash for sustainable geopolymer: A review,” *Constr. Build. Mater.*, vol. 310, no. August, p. 125218, 2021, doi: 10.1016/j.conbuildmat.2021.125218.

[134] A. S. and J. S. K. K. 1Dhirajlal B.Prabu, “A review on rick husk ash based geopolymer concrete,” vol. 3, no. January, pp. 288–294, 2018, [Online]. Available: https://www.researchgate.net/publication/324603174

[135] R. H. Geraldo, L. F. R. Fernandes, and G. Camarini, “Water treatment sludge and rice husk ash to sustainable geopolymer production,” *J. Clean. Prod.*, vol. 149, pp. 146–155, 2017, doi: 10.1016/j.jclepro.2017.02.076.

[136] A. N. Sari, E. Srisunarsih, and T. L. A. Sucipto, “The Use of Rice Husk Ash in Enhancing the Material Properties of Fly Ash-Based Self Compacted Geopolymer Concrete,” *IOP Conf. Ser. Earth Environ. Sci.*, vol. 1808, no. 1, 2021, doi: 10.1088/1742-6596/1808/1/012011.

[137] M. Z. Zaidahtulakmal, K. Kartini, and M. S. Hamidah, “Rice husk ash (RHA) based geopolymer mortar incorporating sewage sludge ash (SSA),” *J. Phys. Conf. Ser.*, vol. 1349, no. 1, 2019, doi: 10.1088/1742-6596/1349/1/012022.

[138] M. S. M. Basri, F. Mustapha, N. Mazlan, and M. R. Ishak, “Rice husk ash-based geopolymer binder: Compressive strength, optimize composition, FTIR spectroscopy, microstructural, and potential as fire-retardant material†,” *Polymers (Basel).*, vol. 13, no. 24, 2021, doi: 10.3390/polym13244373.

[139] H. K. Tchakouté, C. H. Rüscher, S. Kong, E. Kamseu, and C. Leonelli, “Geopolymer binders from metakaolin using sodium waterglass from waste glass and rice husk ash as alternative activators: A comparative study,” *Constr. Build. Mater.*, vol. 114, pp. 276–289, 2016, doi: 10.1016/j.conbuildmat.2016.03.184.

[140] R. Premkumar, P. Hariharan, and S. Rajesh, “Effect of silica fume and recycled concrete aggregate on the mechanical properties of GGBS based geopolymer concrete,” *Mater. Today Proc.*, vol. 60, pp. 211–215, 2022, doi: 10.1016/j.matpr.2021.12.442.

[141] A. J. Daniel, S. Sivakamasundari, and A. Nishanth, “Study on Partial Replacement of Silica Fume Based Geopolymer Concrete Beam Behavior under Torsion,” *Procedia Eng.*, vol. 173, pp. 732–739, 2017, doi: 10.1016/j.proeng.2016.12.162.

[142] R. P. Singh, K. R. Vanapalli, V. R. S. Cheela, S. R. Peddireddy, H. B. Sharma, and B. Mohanty, “Fly ash, GGBS, and silica fume based geopolymer concrete with recycled aggregates: Properties and environmental impacts,” *Constr. Build. Mater.*, vol. 378, no. January, p. 131168, 2023, doi: 10.1016/j.conbuildmat.2023.131168.

[143] F. N. Okoye, S. Prakash, and N. B. Singh, “Durability of fly ash based geopolymer concrete in the presence of silica fume,” *J. Clean. Prod.*, vol. 149, pp. 1062–1067, 2017, doi: 10.1016/j.jclepro.2017.02.176.

[144] N. Billong, J. Oti, and J. Kinuthia, “Using silica fume based activator in sustainable geopolymer binder for building application,” *Constr. Build. Mater.*, vol. 275, p. 122177,

2021, doi: 10.1016/j.conbuildmat.2020.122177.

[145] F. N. Okoye, J. Durgaprasad, and N. B. Singh, “Effect of silica fume on the mechanical properties of fly ash based-geopolymer concrete,” *Ceram. Int.*, vol. 42, no. 2, pp. 3000–3006, 2016, doi: 10.1016/j.ceramint.2015.10.084.

[146] Y. R. Hamed, M. M. Yousry Elshikh, A. A. Elshami, M. H. S. Matthana, and O. Youssf, “Mechanical properties of fly ash and silica fume based geopolymer concrete made with magnetized water activator,” *Constr. Build. Mater.*, vol. 411, no. December 2023, p. 134376, 2024, doi: 10.1016/j.conbuildmat.2023.134376.

[147] S. Park, J. Yu, J. E. Oh, and S. Pyo, “Effect of Silica Fume on the Volume Expansion of Metakaolin-Based Geopolymer Considering the Silicon-to-Aluminum Molar Ratio,” *Int. J. Concr. Struct. Mater.*, vol. 16, no. 1, 2022, doi: 10.1186/s40069-022-00510-2.

[148] R. Bajpai, K. Choudhary, A. Srivastava, K. S. Sangwan, and M. Singh, “Environmental impact assessment of fly ash and silica fume based geopolymer concrete,” *J. Clean. Prod.*, vol. 254, p. 120147, 2020, doi: 10.1016/j.jclepro.2020.120147.

[149] P. S. Deb, P. K. Sarker, and S. Barbhuiya, “Sorptivity and acid resistance of ambient-cured geopolymer mortars containing nano-silica,” *Cem. Concr. Compos.*, vol. 72, pp. 235–245, 2016, doi: 10.1016/j.cemconcomp.2016.06.017.

[150] L. G. Baltazar, “Performance of Silica Fume-Based Geopolymer Grouts for Heritage Masonry Consolidation,” *Crystals*, vol. 12, no. 2, 2022, doi: 10.3390/cryst12020288.

[151] J. N. Y. Djobo, A. Elimbi, H. K. Tchakouté, and S. Kumar, “Volcanic ash-based geopolymer cements/concretes: the current state of the art and perspectives,” *Environ. Sci. Pollut. Res.*, vol. 24, no. 5, pp. 4433–4446, 2017, doi: 10.1007/s11356-016-8230-8.

[152] A. M. Zeyad, H. M. Magbool, B. A. Tayeh, A. R. Garcez de Azevedo, A. Abutaleb, and Q. Hussain, “Production of geopolymer concrete by utilizing volcanic pumice dust,” *Case Stud. Constr. Mater.*, vol. 16, no. November 2021, p. e00802, 2022, doi: 10.1016/j.cscm.2021.e00802.

[153] H. Tchakoute Kouamo, J. A. Mbey, A. Elimbi, B. B. Kenne Diffo, and D. Njopwouo, “Synthesis of volcanic ash-based geopolymer mortars by fusion method: Effects of adding metakaolin to fused volcanic ash,” *Ceram. Int.*, vol. 39, no. 2, pp. 1613–1621, 2013, doi: 10.1016/j.ceramint.2012.08.003.

[154] J. V. Sontia Metekong *et al.*, “Evaluation of performances of volcanic-ash-laterite based blended geopolymer concretes: Mechanical properties and durability,” *J. Build. Eng.*, vol. 34, no. August 2019, 2021, doi: 10.1016/j.jobe.2020.101935.

[155] E. Barrie *et al.*, “Potential of inorganic polymers (geopolymers) made of halloysite and volcanic glass for the immobilisation of tailings from gold extraction in Ecuador,” *Appl. Clay Sci.*, vol. 109–110, pp. 95–106, 2015, doi: 10.1016/j.clay.2015.02.025.

[156] J. N. Yankwa Djobo, A. Elimbi, H. Kouamo Tchakouté, and S. Kumar, “Mechanical properties and durability of volcanic ash based geopolymer mortars,” *Constr. Build. Mater.*, vol. 124, pp. 606–614, 2016, doi: 10.1016/j.conbuildmat.2016.07.141.

[157] A. M. Zeyad, B. A. Tayeh, and M. O. Yusuf, “Strength and transport characteristics of volcanic pumice powder based high strength concrete,” *Constr. Build. Mater.*, vol. 216, pp. 314–324, 2019, doi: 10.1016/j.conbuildmat.2019.05.026.

[158] S. Al-Fadala, J. Chakkamalayath, S. Al-Bahar, A. Al-Aibani, and S. Ahmed, “Significance of performance based specifications in the qualification and characterization of blended cement using volcanic ash,” *Constr. Build. Mater.*, vol. 144, pp. 532–540, 2017, doi: 10.1016/j.conbuildmat.2017.03.180.

[159] A. Kiliç and Z. Sertabipoılu, “Effect of heat treatment on pozzolanic activity of volcanic pumice used as cementitious material,” *Cem. Concr. Compos.*, vol. 57, pp. 128–132, 2015, doi: 10.1016/j.cemconcomp.2014.12.006.

[160] D. M. Roy, G. R. Gouda, and A. Bobrowsky, “Very high strength cement pastes prepared by hot pressing and other high pressure techniques,” *Cem. Concr. Res.*, vol. 2, no. 3, pp. 349–366, 1972, doi: 10.1016/0008-8846(72)90075-0.

[161] P. Posi, S. Lertnimoolchai, V. Sata, and P. Chindaprasirt, “Pressed lightweight concrete containing calcined diatomite aggregate,” *Constr. Build. Mater.*, vol. 47, pp. 896–901, 2013, doi: 10.1016/j.conbuildmat.2013.05.094.

[162] H. Eskandari-Naddaf and M. Azimi-Pour, “Performance evaluation of dry-pressed concrete curbs with variable cement grades by using Taguchi method,” *Ain Shams Eng. J.*, vol. 9, no. 4, pp. 1357–1364, 2018, doi: 10.1016/j.asej.2016.09.004.

[163] S. Sumarni and W. Wijanarko, “Preparation and Mechanical Properties of Pressed Straw Concrete Brick,” *IOP Conf. Ser. Mater. Sci. Eng.*, vol. 333, no. 1, 2018, doi:

10.1088/1757-899X/333/1/012098.

[164] N. Ranjbar, M. Mehrali, M. R. Maheri, and M. Mehrali, “Hot-pressed geopolymer,” *Cem. Concr. Res.*, vol. 100, no. October 2016, pp. 14–22, 2017, doi: 10.1016/j.cemconres.2017.05.010.

[165] H. Wang, L. Wang, Y. Song, and J. Wang, “Influence of free water on dynamic behavior of dam concrete under biaxial compression,” *Constr. Build. Mater.*, vol. 112, pp. 222–231, 2016, doi: 10.1016/j.conbuildmat.2016.02.090.

[166] Y. Cao, J. Ma, C. Lin, M. Yang, S. Xu, and L. Pan, “Feasibility of developing strain-hardening geopolymer composite plates by hot-pressing method,” *Cem. Concr. Compos.*, vol. 138, no. January, p. 104956, 2023, doi: 10.1016/j.cemconcomp.2023.104956.

[167] D. M. Roy and G. R. Gouda, “High strength generation in cement pastes,” *Cem. Concr. Res.*, vol. 3, no. 6, pp. 807–820, 1973, doi: 10.1016/0008-8846(73)90013-6.

[168] T. Mangialardi, “Sintering of MSW fly ash for reuse as a concrete aggregate,” *J. Hazard. Mater.*, vol. 87, no. 1–3, pp. 225–239, 2001, doi: 10.1016/S0304-3894(01)00286-2.

[169] P. Xue *et al.*, “Research on the sintering process and characteristics of belite sulphoaluminate cement produced by BOF slag,” *Constr. Build. Mater.*, vol. 122, pp. 567–576, 2016, doi: 10.1016/j.conbuildmat.2016.06.098.

[170] L. Zingg, M. Briffaut, J. Baroth, and Y. Malecot, “Influence of cement matrix porosity on the triaxial behaviour of concrete,” *Cem. Concr. Res.*, vol. 80, pp. 52–59, 2016, doi: 10.1016/j.cemconres.2015.10.005.

[171] Z. Wu, K. H. Khayat, and C. Shi, “Changes in rheology and mechanical properties of ultra-high performance concrete with silica fume content,” *Cem. Concr. Res.*, vol. 123, no. June, p. 105786, 2019, doi: 10.1016/j.cemconres.2019.105786.

[172] G. Goglio, A. Ndayishimiye, C. Elissalde, and C. A. Randall, “Cold sintering and hydrothermal sintering,” *Encycl. Mater. Tech. Ceram. Glas.*, vol. 1–3, pp. 311–326, 2021, doi: 10.1016/B978-0-12-803581-8.12113-7.

[173] M. Zahabi, A. Said, and A. Memari, “Cold Sintering of Calcium Carbonate for Construction Material Applications,” *ACS Omega*, vol. 6, no. 4, pp. 2576–2588, 2021, doi: 10.1021/acsomega.0c04617.

[174] P. Posi *et al.*, "Preliminary study of pressed lightweight geopolymer block using fly ash, Portland cement and recycled lightweight concrete," *Key Eng. Mater.*, vol. 718, pp. 184–190, 2017, doi: 10.4028/www.scientific.net/KEM.718.184.

[175] S. Wang, X. Ma, L. He, Z. Zhang, L. Li, and Y. Li, "High strength inorganic-organic polymer composites (IOPC) manufactured by mold pressing of geopolymers," *Constr. Build. Mater.*, vol. 198, pp. 501–511, 2019, doi: 10.1016/j.conbuildmat.2018.11.281.

[176] V. Carvelli *et al.*, "Low-velocity impact of hot-pressed PVA fiber-reinforced alkali-activated stone wool composites," *Cem. Concr. Compos.*, vol. 114, no. September, p. 103805, 2020, doi: 10.1016/j.cemconcomp.2020.103805.

[177] H. Nguyen *et al.*, "Fiber reinforced alkali-activated stone wool composites fabricated by hot-pressing technique," *Mater. Des.*, vol. 186, p. 108315, 2020, doi: 10.1016/j.matdes.2019.108315.

[178] N. Ranjbar, A. Kashefi, G. Ye, and M. Mehrali, "Effects of heat and pressure on hot-pressed geopolymer," *Constr. Build. Mater.*, vol. 231, p. 117106, 2020, doi: 10.1016/j.conbuildmat.2019.117106.

[179] K. Nishikawa, K. Yamaguchi, T. Suzuki, S. Hashimoto, and S. Rossignol, "Effect of amorphous silica fume as active filler for rapid densification of the geopolymer products formed by warm pressing," *Ceram. Int.*, vol. 48, no. 24, pp. 36917–36924, 2022, doi: 10.1016/j.ceramint.2022.08.258.

[180] S. Prasanphan, A. Wannagon, T. Kobayashi, and S. Jiemsirilers, "Microstructure evolution and mechanical properties of calcined kaolin processing waste-based geopolymers in the presence of different alkali activator content by pressing and casting," *J. Met. Mater. Miner.*, vol. 30, no. 3, pp. 121–132, 2020, doi: 10.14456/jmmm.2020.45.

[181] O. Shee Ween, H. Cheng-Yong, M. Mustafa Al Bakri Abdullah, L. N. Ho, and O. Wan En, "Geopolymer via Pressing Method: Aluminosilicates/Alkaline Solution Ratio as the Determining Factor," *IOP Conf. Ser. Mater. Sci. Eng.*, vol. 864, no. 1, 2020, doi: 10.1088/1757-899X/864/1/012164.

[182] K. Nishikawa, S. Hashimoto, H. Imai, and S. Rossignol, "Cold reaction sintering for preparation of ultra-dense geopolymer products," *Constr. Build. Mater.*, vol. 328, no.

October 2021, p. 127101, 2022, doi: 10.1016/j.conbuildmat.2022.127101.

[183] O. Shee-Ween *et al.*, "Cold-pressed fly ash geopolymers: effect of formulation on mechanical and morphological characteristics," *J. Mater. Res. Technol.*, vol. 15, pp. 3028–3046, 2021, doi: 10.1016/j.jmrt.2021.09.084.

[184] N. Li, C. Shi, Z. Zhang, H. Wang, and Y. Liu, "A review on mixture design methods for geopolymer concrete," *Compos. Part B Eng.*, vol. 178, no. April, p. 107490, 2019, doi: 10.1016/j.compositesb.2019.107490.

[185] IS 383 : 2016, "Specification for Coarse and Fine Aggregates From Natural Sources for Concrete," *Bureau of Indian Standards,New Delhi*. pp. 1–24, 2016.

[186] IS 10262 : 2019, "Indian standard, Concrete mix Proportioning – Guidelines (Second Revision).," *Bis*, no. January, pp. 1–42, 2019.

[187] IS 17452 : 2020, "Use of Alkali Activated Concrete for Precast Products-Guidelines," vol. 86, no. December, pp. 34–117, 2020, [Online]. Available: www.standardsbis.in

[188] IS 516 (Part 1/Sec 1) : 2021, "Method of Tests for Strength of Concrete," *Bur. Indian Stand.*, vol. 516, no. March, pp. 1–30, 2021.

[189] IS 516 : Part 5 (Section 4), "Hardened concrete - Methods of test," *Is*, vol. 54, no. August, pp. 1–20, 2021, [Online]. Available: www.standardsbis.in

[190] IS 516 : Part 5 (Section 1), "Hardened Concrete — Methods of Test - Testing of Strength of Hardened Concrete," *Bur. Indian Stand. New Delhi*, vol. 516, no. August, 2018.

[191] ASTM C1585-04, "Standard Test Method for Measurement of Rate of Absorption of Water by Hydraulic-Cement Concretes", [Online]. Available: Standard Test Method for Measurement of Rate of Absorption of Water by Hydraulic-Cement Concretes

[192] ASTM C1202-12, "Standard Test Method for Electrical Indication of Concrete's Ability to Resist Chloride Ion Penetration." https://www.astm.org/standards/c1202

[193] S. Gargepuram, S. Subash, and S. Moharana, "Pore Evaluation and Distribution in Cement Mortar Using Digital Image Processing," *Lect. Notes Mech. Eng.*, no. February, pp. 125–131, 2021, doi: 10.1007/978-981-16-0186-6_13.

[194] N. Zabihi, "Effect of Specimen Size and Shape on Strength of Concrete.," no. January, 2012, doi: 10.13140/RG.2.2.17927.83360.

[195] J. Bates, *Zero Carbon Industry Plan : Rethinking Cement*. 2017.

[196] E. Gartner and H. Hirao, “A review of alternative approaches to the reduction of CO2 emissions associated with the manufacture of the binder phase in concrete,” *Cem. Concr. Res.*, vol. 78, pp. 126–142, 2015, doi: 10.1016/j.cemconres.2015.04.012.

[197] E. Gartner, “Industrially interesting approaches to ‘low-CO2’ cements,” *Cem. Concr. Res.*, vol. 34, no. 9, pp. 1489–1498, 2004, doi: 10.1016/j.cemconres.2004.01.021.